

This discussion paper is/has been under review for the journal *Atmospheric Chemistry and Physics (ACP)*. Please refer to the corresponding final paper in *ACP* if available.

# Comparison of OMI NO<sub>2</sub> tropospheric columns with an ensemble of global and European regional air quality models

V. Huijnen<sup>1</sup>, H. J. Eskes<sup>1</sup>, B. Amstrup<sup>2</sup>, R. Bergstrom<sup>3</sup>, K. F. Boersma<sup>1</sup>,  
H. Elbern<sup>4</sup>, J. Flemming<sup>5</sup>, G. Foret<sup>6</sup>, E. Friese<sup>4</sup>, A. Gross<sup>2</sup>, M. D'Isidoro<sup>7</sup>,  
I. Kioutsioukis<sup>8</sup>, A. Maurizi<sup>7</sup>, D. Melas<sup>8</sup>, V.-H. Peuch<sup>9</sup>, A. Poupkou<sup>8</sup>,  
L. Robertson<sup>3</sup>, M. Sofiev<sup>10</sup>, O. Stein<sup>11,12</sup>, A. Strunk<sup>4</sup>, A. Valdebenito<sup>13</sup>,  
C. Zerefos<sup>8</sup>, and D. Zyryanov<sup>6,14</sup>

<sup>1</sup>Royal Netherlands Meteorological Institute, De Bilt, The Netherlands

<sup>2</sup>Danish Meteorological Institute, Copenhagen, Denmark

<sup>3</sup>Swedish Meteorological and Hydrological Institute, Norrköping, Sweden

<sup>4</sup>Rhenish Institute for Environmental Research at the University of Cologne, Köln, Germany

<sup>5</sup>European Centre for Medium-Range Weather Forecasts (ECMWF), Reading, UK

<sup>6</sup>Laboratoire Interuniv. des Systèmes Atmosphériques, CNRS/Univ. Paris 12 et 7, Créteil, France

<sup>7</sup>Institute of Atmospheric Sciences and Climate, Consiglio Nazionale delle Ricerche, Bologna, Italy

**Comparison of NO<sub>2</sub>  
in regional and global  
models to OMI**

V. Huijnen et al.

Title Page

Abstract

Introduction

Conclusions

References

Tables

Figures

◀

▶

◀

▶

Back

Close

Full Screen / Esc

Printer-friendly Version

Interactive Discussion



---

**Comparison of NO<sub>2</sub>  
in regional and global  
models to OMI**V. Huijnen et al.

---

[Title Page](#)[Abstract](#)[Introduction](#)[Conclusions](#)[References](#)[Tables](#)[Figures](#)[I◀](#)[▶I](#)[◀](#)[▶](#)[Back](#)[Close](#)[Full Screen / Esc](#)[Printer-friendly Version](#)[Interactive Discussion](#)

<sup>8</sup>Laboratory of Climatology, Faculty of Geology, University of Athens, Athens, Greece

<sup>9</sup>CNRM-GAME, Météo-France and CNRS URA 1357, Toulouse, France

<sup>10</sup>Air Quality Research, Finnish Meteorological Institute, Finland

<sup>11</sup>Institute for Chemistry and Dynamics of the Geosphere (ICG), FZ Jülich, Germany

<sup>12</sup>Max Planck Institute for Meteorology, Hamburg, Germany

<sup>13</sup>Norwegian Meteorological Institute, Norway

<sup>14</sup>Laboratoire de Météorologie Dynamique, CNRS/IPSL, Ecole polytechnique, Palaiseau, France

Received: 20 August 2009 – Accepted: 6 October 2009 – Published: 22 October 2009

Correspondence to: V. Huijnen (huijnen@knmi.nl)

## Abstract

We present model results for tropospheric NO<sub>2</sub> from 9 regional models and 2 global models that are part of the GEMS-RAQ forecast system, for July 2008 to June 2009 over Europe. These modeled NO<sub>2</sub> columns are compared with OMI NO<sub>2</sub> satellite retrievals and surface observations from the Dutch Air Quality Network. The participating models apply principally the same emission inventory, but vary in model resolution (0.15 to 0.5°), chemical mechanism, meteorology and transport scheme. For area-averaged columns only a small bias is found when the averaging kernel is neglected in the comparison to OMI NO<sub>2</sub> columns. The reason for this is that TM4 a priori profiles have higher NO<sub>x</sub> concentrations in the free troposphere (where sensitivity to NO<sub>2</sub> is high) and higher NO<sub>x</sub> concentrations in the surface layers (where sensitivity to NO<sub>2</sub> is low) than RAQ models, effectively cancelling the effect of applying the averaging kernel. We attribute these low NO<sub>2</sub> concentrations in the RAQ models to missing emissions from aircraft and lightning. It is also shown that the NO<sub>2</sub> concentrations from the upper part of the troposphere (higher than 500 hPa) contribute up to 20% of the total tropospheric NO<sub>2</sub> signal observed by OMI. Compared to the global models the RAQ models show a better correlation to the OMI NO<sub>2</sub> observations, which are characterized by high spatial variation due to the short lifetime for NO<sub>2</sub>. The spread in the modeled tropospheric NO<sub>2</sub> column is on average 20–40%. In summer the mean of all models is on average 46% below the OMI observations, whereas in winter the models are more in line with OMI. On the other hand the models on average under-predict surface concentrations in winter by 24% and are more in line with observations in summer. These findings suggest that OMI tropospheric columns in summer over polluted regions are biased high by about 40%. The diurnal cycle and profiles in the regional models are well in line, and the profile shapes correspond well to results from the global models. The analyses against OMI observations have proven to be very useful to initiate model improvements, and to quantify uncertainties in the retrieval product.

### Comparison of NO<sub>2</sub> in regional and global models to OMI

V. Huijnen et al.

Title Page

Abstract

Introduction

Conclusions

References

Tables

Figures

◀

▶

◀

▶

Back

Close

Full Screen / Esc

Printer-friendly Version

Interactive Discussion



## 1 Introduction

NO<sub>2</sub> is a key chemical variable determining air quality. It affects human health directly, and indirectly through increased ozone concentrations (Godowitch et al., 2008), as NO<sub>2</sub> acts as a catalyst in ozone formation Knowlton et al. (2004). The trace gases relevant for regional air quality are affected by local sources and weather conditions, but also by changing background conditions influenced by long range transport of pollution from elsewhere. Studies have shown that a change in emission levels causing changes in climate can counteract, or enhance changes in the regional air quality, e.g. Huang et al. (2008), Nolte et al. (2008), Chen et al. (2009).

Regional air quality (RAQ) models have been developed in many countries to describe and forecast surface concentrations of health-related species, such as O<sub>3</sub>, aerosols and NO<sub>x</sub>. As the quality of the RAQ models improves, their use in an operational system for the provision of daily forecasts of regional composition of the atmosphere comes within reach. There are already several examples of models that are delivering such air quality forecasts on an operational, regular basis, for instance, the French Prevoir system (Rouil et al., 2009), or the US AIRNow system (<http://www.airnow.gov>). NO<sub>2</sub> is one of the key trace gases that is extensively tracked.

The European project “Global and regional Earth-system (atmosphere) Monitoring using Satellite and in-situ data” (GEMS) aimed at developing a pre-operational system for forecasting the chemical composition of the atmosphere, both on a global scale and on a regional scale for Europe, using an ensemble of RAQ models (Hollingsworth et al., 2008). As part of this project a number of RAQ models have been set up independently to deliver forecasts of trace gases on a daily basis, up to three days ahead. These are the models BOLCHEM (Mircea et al., 2008), CAC (Gross et al., 2007), CAMx (Morris et al., 2003) CHIMERE (Bessagnet et al., 2008), EMEP (Simpson et al., 2003), EURAD-IM (Elbern et al., 2007), MATCH (Andersson et al., 2007), MOCAGE (Josse et al., 2004), (Bousserez et al., 2007), NAME-AQ (Jones et al., 2007) and SILAM (Sofiev et al., 2008a). Three global Chemistry Transport Models (CTMs)

### Comparison of NO<sub>2</sub> in regional and global models to OMI

V. Huijnen et al.

Title Page

Abstract

Introduction

Conclusions

References

Tables

Figures

◀

▶

◀

▶

Back

Close

Full Screen / Esc

Printer-friendly Version

Interactive Discussion



are also contributing. The MOZART model (Horowitz et al., 2003; Kinnison et al., 2007) was coupled to ECMWF's integrated forecast system (IFS) resulting in the MOZART-IFS forecast system (Flemming et al., 2009). This model delivers daily forecasts for reactive trace gases, which are used in several RAQ models for their trace gas boundary conditions. The models MOCAGE (Josse et al., 2004; Boussez et al., 2007) and TM5 (Krol et al., 2005) have been running in an offline mode and (in experimental phase) in a forecast mode coupled to IFS (Flemming et al., 2009).

The models apply basically the same emission inventory, but they differ significantly with respect to the applied chemical mechanisms, transport schemes and meteorological processes. This diversity is an important motivation for the multi-model ensemble forecast approach in the GEMS project. Validation and intercomparison studies such as the one presented here can help to assess and explain differences in the modeled trace gas concentrations and to identify implementation errors. But this large diversity also implies that firm conclusions on origins of more subtle differences are hard to draw.

The RAQ models are routinely verified against surface observations of trace gases and OMI NO<sub>2</sub> satellite observations, see also the gems-website, <http://gems.ecmwf.int/d/products/raq>. Although the verification against surface observations is most relevant from the perspective of the user of local air quality forecasts, there are considerable problems with this type of validation, mainly concerning the representativity, coverage and the measurement accuracy of the surface observations. Complementary to the surface observations, satellite data can give valuable insight in the quality of the models, because it typically provides a complete coverage and contains information on summed concentrations in the boundary layer and the free troposphere.

In previous studies satellite data have been used to validate global CTM's. For instance, van Noije et al. (2006) have performed a model-intercomparison for NO<sub>2</sub> on a global scale, based on GOME retrievals. In their study both the retrievals and the models were smoothed to a common 5×5° grid. It highlighted the differences in the models, but also showed significant differences between the retrieval algorithms.

## Comparison of NO<sub>2</sub> in regional and global models to OMI

V. Huijnen et al.

Title Page

Abstract

Introduction

Conclusions

References

Tables

Figures

◀

▶

◀

▶

Back

Close

Full Screen / Esc

Printer-friendly Version

Interactive Discussion



A more detailed analysis on a  $0.5^\circ$  grid for a regional model (CHIMERE) using the SCIAMACHY  $\text{NO}_2$  data and surface observations was presented by Blond et al. (2007). In these studies some of the differences between models as well as differences of models compared to  $\text{NO}_2$  retrievals remain unclarified. For instance, the effect of the model resolution, related to the large spatial/temporal gradients and the short lifetime of  $\text{NO}_2$  has not been considered.

Also the use of the averaging kernel has an impact when the model profile shape is different from the a priori profile used in the satellite retrieval (Eskes and Boersma, 2003). The intercomparison of RAQ models, that are focussed on surface concentrations, and global CTM's, which are designed to model reasonable background concentrations in the free troposphere, can also be used to quantify this type of model limitations.

In the analysis of modeled tropospheric columns the  $\text{NO}_2$  contribution from the free troposphere needs to be accounted for (Napelenok et al., 2008). Additionally, when using the averaging kernel from the retrieval more weight is given to modeled  $\text{NO}_2$  in the free troposphere, as the satellite is more sensitive to  $\text{NO}_2$  at these levels. Therefore the combination of model validation against both surface observations and satellite retrievals helps to attribute model errors at different levels.

In this study we compare the tropospheric  $\text{NO}_2$  column data derived from the OMI satellite instrument, the DOMINO product version 1.0.2 (Boersma et al., 2007), to the forecasts for  $\text{NO}_2$  from regional and global models that participate in the GEMS project. The DOMINO product was validated successfully in a host of studies, e.g. (Boersma et al., 2008, 2009b; Brinksma et al., 2008) and contains the averaging kernel as well as the a priori profile shapes. OMI achieves an optimum resolution of  $13 \times 24 \text{ km}^2$ , with a daily global coverage. This makes the data very suitable for the daily comparison to the high-resolution RAQ model predictions (with a typical resolution of  $0.2 \times 0.2^\circ$ ). Because of its daily coverage a sufficient amount of data is available for a quantitative, statistical analysis on a monthly basis.

Eight members of the RAQ ensemble have been providing tropospheric  $\text{NO}_2$  con-

## Comparison of $\text{NO}_2$ in regional and global models to OMI

V. Huijnen et al.

Title Page

Abstract

Introduction

Conclusions

References

Tables

Figures

◀

▶

◀

▶

Back

Close

Full Screen / Esc

Printer-friendly Version

Interactive Discussion



centration fields on an hourly basis. We intercompare these model results in terms of total columns, profile shape and surface concentrations from July 2008 to June 2009 over the European domain. The impact of averaging kernels to modeled columns is assessed, in relation to the vertical profiles. Additionally the models are compared against surface observations from the Dutch Air Quality Monitoring Network (LML), Beijk et al. (2007).

An analysis of NO<sub>2</sub> from two global models, MOZART-IFS and TM5, is also included. This gives information on the consistency between the regional and global models, and the effect of using a limited domain in the RAQ models, versus a limited resolution in the global models. A sensitivity study with TM5, with the use of a regional 1×1° resolution over the EU-RAQ domain, versus a global 3×2° baseline version is used to investigate the resolution issue in more detail.

## 2 Participating models

In this section we describe the 10 models, which are all participating in the EU-GEMS project. These include two global models (MOZART-IFS and TM5), and eight RAQ models.

### 2.1 Regional models

The contributing models for this evaluation are BOLCHEM (Mircea et al., 2008), CAC (Gross et al., 2007), CAMx (Morris et al., 2003) CHIMERE (Bessagnet et al., 2008), EMEP (Simpson et al., 2003), EURAD-IM (Elbern et al., 2007), MATCH (Andersson et al., 2007) and SILAM (Sofiev et al., 2008a). A model specification is provided in Table 6. All models deliver tropospheric NO<sub>2</sub> columns on an hourly basis, up to 72 h forecast time. The model domain ranges from -15 to 35° longitude and 35 to 70° latitude. The RAQ models differ substantially in resolution (0.15–0.5°), model height (100–500 hPa), meteorology, chemical mechanism and transport scheme. Four mod-

## Comparison of NO<sub>2</sub> in regional and global models to OMI

V. Huijnen et al.

Title Page

Abstract

Introduction

Conclusions

References

Tables

Figures

◀

▶

◀

▶

Back

Close

Full Screen / Esc

Printer-friendly Version

Interactive Discussion



els directly use meteorology from the IFS operational forecasts, whereas EURAD-IM and CAMx use the MM5 model (Kain, 2002). BOLCHEM uses the BOLAM meteorological model and CAC uses HIRLAM. All these regional meteorological models use initial and boundary values provided by the operational IFS forecast.

5 The chemical mechanisms in CAC and CAMx are based on updated versions of the CBM-IV mechanism (Gery et al., 1989). CHIMERE uses the MELCHIOR II mechanism, (Schmidt et al., 2001), which consists of 44 reactions for 116 gaseous species. The hydrocarbon degradation in MELCHIOR II is similar to the EMEP gas phase mechanism (Simpson et al., 1993). Adaptations are made in particular for low  $\text{NO}_x$  conditions and  $\text{NO}_x$  – nitrate chemistry. BOLCHEM applies the SAPRC90 gas chemistry mechanism (Carter, 1990). The EURAD-IM model applies a 3-D-var data assimilation procedure before the beginning of a forecast, which uses  $\text{NO}_2$  concentrations from measurement sites. Most of the RAQ models except for CAC and EMEP use boundary conditions for trace gases (horizontally and at model top) from the MOZART-IFS forecast system. The EMEP model applies climatological data for most species, and a constant boundary value for  $\text{O}_3$  of 40 ppb.

## 2.2 Global models

20 The MOZART-IFS forecast run experiment ez2m, Flemming et al. (2009) is based on MOZART-3, (Kinnison et al., 2007; Horowitz et al., 2003), coupled to ECMWF's Integrated Forecasting System (IFS). The advective scheme is based on a numerically fast, flux form semi-Lagrangian transport scheme (Lin and Rood, 1996). The chemical mechanism contains the chemical families  $\text{O}_x$ ,  $\text{NO}_x$ ,  $\text{HO}_x$ ,  $\text{ClO}_x$  and  $\text{BrO}_x$ , as well as  $\text{CH}_4$  and a series of non-methane hydrocarbons (NMHCs). In total there are about 108 species, over 200 gas-phase reactions and 70 photolytic processes (Horowitz et al., 2003; Kinnison et al., 2007). The current version applies a gaussian grid with a resolution of about  $1.875^\circ$  longitude/latitude and a distribution of 60 layers, with the top layer at 0.1 hPa. This system has run continuously from January 2008 to April 2009, delivering global forecasts of trace gases up to three days ahead. This experiment is

---

### Comparison of $\text{NO}_2$ in regional and global models to OMI

V. Huijnen et al.

---

Title Page

Abstract

Introduction

Conclusions

References

Tables

Figures

◀

▶

◀

▶

Back

Close

Full Screen / Esc

Printer-friendly Version

Interactive Discussion



based on a free-running coupled system, i.e. without data assimilation.

The TM5 model, (Krol et al., 2005), version KNMI-cy3-GEMS is employed offline, and uses the operational meteorological fields from ECMWF. The baseline horizontal resolution is  $3 \times 2^\circ$  longitude/latitude. In the current setup the model has 34 vertical layers with the top layer at 0.1 hPa. The chemistry scheme in TM5 is based on a modified CBM-IV mechanism (Gery et al., 1989; Houweling et al., 1998). The main modifications concern an extension of the methane oxidation chemistry and updating the product distribution for the isoprene oxidation reactions. This improves the performance for background conditions, (Houweling et al., 1998). The rate constants have been updated to the latest recommendations from JPL (Sander et al., 2006), which result in an improved agreement for CO at remote locations (Williams et al., 2008). Tracer advection is evaluated with the “slopes” scheme (Russell and Lerner, 1981), and convective transport is according to Holtslag and Boville (1993). Another difference compared to the standard version of TM5 is that transport of NO<sub>2</sub> and NO is evaluated explicitly, rather than using a scaling by NO<sub>x</sub>. For this study model runs were performed with the baseline resolution as well as with a zoom region with a resolution over Europe of  $1 \times 1^\circ$ . These model runs are denoted as TM5 and TM5-Zoom, respectively. Both in TM5 and MOZART-IFS the NO<sub>x</sub> emissions are injected in the model as NO. The tropospheric column is evaluated based on a definition for the tropopause where O<sub>3</sub> exceeds 150 ppb. Above Europe this is at about 200 hPa.

### 2.3 NO<sub>x</sub> Emissions

The emission inventory in all the RAQ models is based on the TNO inventory for 2003 created specifically for GEMS, (Visschedijk et al., 2007; Visschedijk and van der Gon, 2005). Only the EMEP model uses the EMEP 2003 emission inventory (Tarrasón et al., 2005). This inventory provides emissions on a high spatial resolution ( $1/8 \times 1/16^\circ$  longitude / latitude, i.e. approximately  $7 \times 7$  km), based on official emission data on a country-basis that has been submitted to EMEP/CLRTAP (Wagner et al., 2005). It makes distinction between surface sources and point-sources, which may be injected into higher

## Comparison of NO<sub>2</sub> in regional and global models to OMI

V. Huijnen et al.

Title Page

Abstract

Introduction

Conclusions

References

Tables

Figures

◀

▶

◀

▶

Back

Close

Full Screen / Esc

Printer-friendly Version

Interactive Discussion



model levels. The total amount of anthropogenic NO<sub>x</sub> emissions for the EU RAQ domain is 4.2 Tg N/yr. The emission inventory in both global models is based on the RETRO-2000 inventory (<http://retro.enes.org>), see Table 1.

In Fig. 1 the yearly-average NO<sub>x</sub> emissions from RETRO and TNO are shown. On average the total NO<sub>x</sub> anthropogenic emissions for RETRO are about 10% higher, due to higher emissions over the Western part of Europe. In this region, the emissions are on average about 2.5 times higher than what is specified by TNO. Over East and South-East Europe the inventories are more alike, and occasionally TNO is higher. This suggests that the emission data from RETRO is outdated for the current evaluation period over these regions. Recently an emission inventory for Greece (Markakis et al., 2009b) and the Greater Istanbul Area (Markakis et al., 2009a) has been compiled based on detailed activity data as well as national emission reports employing bottom-up methodologies. The comparison between these inventories and the TNO inventory indicate a possible underestimation of NO<sub>2</sub> in the TNO inventory of 26% for Greece and 57% for Istanbul, which has seen substantial economic growth in the past ten years.

In SILAM the EMEP inventory, (Tarrasón et al., 2005) has been adapted to fill in the missing emissions in the TNO inventory for some Eastern European and Asian countries. In CAMx, CHIMERE, BOLCHEM, MATCH and SILAM ships-emissions based on the EMEP inventory (Vestreng, 2003) have been included. In contrast to the global CTM's, the regional models apply a diurnal cycle and distinguish between working days and weekends. The temporal disaggregation (monthly/weekly/diurnal) is based on, e.g., the GENEMIS project (Society, 1994). Different to the RAQ models, the global models include parameterizations for lightning NO<sub>x</sub> emissions, aircraft emissions and a climatological emission set for biomass burning. The lighting and aircraft emissions as applied in TM5 are slightly larger than in MOZART-IFS, Table 1. From the RAQ models only the EMEP model includes lightning parametrization for NO<sub>x</sub> emissions, Köhler et al. (1995).

---

## Comparison of NO<sub>2</sub> in regional and global models to OMI

V. Huijnen et al.

---

[Title Page](#)[Abstract](#)[Introduction](#)[Conclusions](#)[References](#)[Tables](#)[Figures](#)[⏪](#)[⏩](#)[◀](#)[▶](#)[Back](#)[Close](#)[Full Screen / Esc](#)[Printer-friendly Version](#)[Interactive Discussion](#)

### 3 The OMI NO<sub>2</sub> product

#### 3.1 DOMINO Product description

OMI has an overpass at approximately 13:30 LT and achieves a resolution of 13 km along track and 24 km in nadir across track, with its highest resolution at small viewing zenith angles. It obtains global coverage within one day, as OMI observes the atmosphere with a 114° field of view corresponding to a 2600 km wide spatial swath. This image is constructed from 60 discrete viewing angles, perpendicular to the flight direction. The OMI datasets are publicly available from the Temis project website (<http://www.temis.nl>).

The retrieval algorithm for the DOMINO product (version 1.0.2) has been described by Boersma et al. (2007, 2009a). Slant columns for NO<sub>2</sub> are retrieved using the differential optical absorption spectroscopy technique (DOAS) in the 405–465 nm range. For the evaluation of tropospheric columns a combined retrieval-assimilation-modelling approach is used. The stratospheric NO<sub>2</sub> columns are obtained by running the TM4 chemistry transport model forward in time based on assimilated NO<sub>2</sub> information from previously observed orbits. For the evaluation of the retrieval air mass factor (AMF) the TM4 model tropospheric NO<sub>2</sub> profiles simulated for 13:30 LT are used. TM4 evaluates the tropospheric composition on a 3×2° resolution and uses basically the same chemical mechanism as in TM5, as described in Houweling et al. (1998). Cloud fraction and cloud pressure are obtained by the O<sub>2</sub>-O<sub>2</sub> algorithm (Acarreta et al., 2004). Prior to 17 February 2009 surface albedo from combined TOMS and GOME sets are used in the standard DOMINO product. After this date this is replaced by a surface albedo map derived from the OMI-database at 471 nm (Kleipool et al., 2008).

For this study the retrieved tropospheric NO<sub>2</sub> columns have been filtered for pixels where cloud radiance fraction is less than 50%, i.e. less than half of the incoming radiation is due to cloud scattering. This roughly corresponds to cloud fractions below 10–20%, which implies that the models are evaluated for (nearly) clear-sky conditions. Note that tropospheric NO<sub>2</sub> is strongly affected by clouds, through large vertical mixing

### Comparison of NO<sub>2</sub> in regional and global models to OMI

V. Huijnen et al.

Title Page

Abstract

Introduction

Conclusions

References

Tables

Figures

◀

▶

◀

▶

Back

Close

Full Screen / Esc

Printer-friendly Version

Interactive Discussion



---

**Comparison of NO<sub>2</sub> in regional and global models to OMI**V. Huijnen et al.

---

[Title Page](#)[Abstract](#)[Introduction](#)[Conclusions](#)[References](#)[Tables](#)[Figures](#)[◀](#)[▶](#)[◀](#)[▶](#)[Back](#)[Close](#)[Full Screen / Esc](#)[Printer-friendly Version](#)[Interactive Discussion](#)

and changes in photo-chemistry. Cloudy low-pressure areas with large advective forcing can be related to long-range horizontal transport of NO<sub>2</sub>, see e.g. (Schaub et al., 2006). These cloud-related effects cannot be investigated with the current OMI product, as the satellite cannot observe below-cloud NO<sub>2</sub> concentrations. In cases where multiple measurements are available at the same location for the same day a weighting of observation data is applied, based on the squared cosine of the satellite viewing zenith angle. In this way high resolution observations are given more weight than observations at the side of the swath. During the analysis period several row anomalies occurred in OMI data. The affected rows have been removed from the data set, see <http://www.temis.nl> and (Boersma et al., 2009a).

The tropospheric NO<sub>2</sub> DOMINO product has been validated against surface, in-situ and aircraft observations, such as during the INTEX-B and DANDELIONS campaigns (Boersma et al., 2008; Brinksma et al., 2008; Hains et al., 2009) and observations in Israel, (Boersma et al., 2009b). In general, the assumption of a well mixed boundary layer at OMI overpass (early afternoon) leads to a satisfactory comparison with surface NO<sub>2</sub> observations, (Boersma et al., 2009b).

### 3.2 Uncertainties in the DOMINO product

The contributions to the error estimate in the tropospheric NO<sub>2</sub> column are described in (Boersma et al., 2004). Here the uncertainty due to cloud fraction (and aerosols) are estimated to be up to 30% for polluted regions and uncertainties due the surface albedo up to 15%. For the retrieval of the vertical NO<sub>2</sub> column an a priori estimate of the NO<sub>2</sub> profile is needed. Errors in the a priori profile shape can be caused by an under-representation of the OMI pixels, due to the low spatial resolution of the a priori concentration field (Boersma et al., 2007). The uncertainty in the tropospheric AMF due to the model profile is evaluated for the GOME retrieval by Boersma et al. (2004), and is estimated of the order of 10%.

Recently it is shown that an improved surface albedo map (Kleipool et al., 2008), leads to an average decrease of the OMI NO<sub>2</sub> columns by about 12% in September

over the Netherlands (Hains et al., 2009). They also found that the DOMINO product in September over the Netherlands is over-estimating the total columns by 10% when using the TM4 profiles, compared to using LIDAR measurement profiles. This is attributed to a too modest mixing of the boundary layer in the TM4 model. For measurement locations in less polluted regions the a priori profile shapes are generally well in line with the observations. A study where TM4 a priori profiles are replaced with GEOS-CHEM profiles (Lamsal et al., 2009), which assumes full mixing in the planetary boundary layer, confirmed these findings. Also Zhou et al. (2009) report a high bias over rural areas in spring and summer over the Swiss Plateau. Another effect that leads to systematic errors in the current DOMINO product concerns the air mass factor (AMF) for the lowest model layer. The interpolation method used results in too low values for the lowest box AMF and consequently 0–20% too high tropospheric NO<sub>2</sub> columns (Zhou et al., 2009). To conclude, combining the above effects suggests that the current OMI product is biased high over polluted regions by 0–40%, especially in summer.

#### 4 Intercomparison approaches

In this study we use the model fields from the first forecast day only, as we are mainly focussing on the general differences of NO<sub>2</sub> between models, rather than their forecast skills over time. Ideally all models should be convoluted with the OMI averaging kernels, before comparing the modeled retrieval equivalents to the DOMINO product. Unfortunately full 3-D information is available only for two RAQ models. Instead the OMI product is directly compared to the modeled total columns, which are readily available. To investigate the effect of the neglect of the averaging kernels on the model results, we have performed a sensitivity test for two RAQ models for which the full 3-D model output is present, see Sect. 8.

For the intercomparison of modeled total columns to the retrieval product, the model data is interpolated in space and time to the OMI measurement points. Specifically, the model data is collocated at the OMI measurement points, which means that implicitly

### Comparison of NO<sub>2</sub> in regional and global models to OMI

V. Huijnen et al.

Title Page

Abstract

Introduction

Conclusions

References

Tables

Figures



Back

Close

Full Screen / Esc

Printer-friendly Version

Interactive Discussion



the same cloud cover selection criteria as for the OMI observations are used. Next, the measurement data and the corresponding model data are regridded onto a common  $0.1 \times 0.1^\circ$  grid.

For the intercomparison to surface observations from the Dutch Air Quality Monitoring Network the model output is interpolated in space and time to the available measurements from all rural sites. All available observations are averaged on a monthly basis.

Seven regions have been defined to facilitate the comparison of the models in different parts over the RAQ domain, see Table 2 and Fig. 2. During winter months there are no retrievals available over the northern part of Europe, due to low solar zenith angles. To intercompare area-averaged statistics for different months, a “mid/southern-Europe” region is defined where all year round OMI data is available. The region over the Netherlands is defined in order to relate the comparison to OMI observations with the analysis at the surface.

Note that in this paper we present  $\text{NO}_2$  data aggregated in different ways, Table 3. For tropospheric  $\text{NO}_2$  the same selection criteria as for the OMI product are adopted. For the comparison to the surface network over The Netherlands the model output is collocated in space and time to the available measurements at 12:00 UTC. For the analysis of the diurnal cycle and the 12:00 UTC profile shapes only a model-intercomparison is performed, therefore all available model data is used for this.

## 5 Comparison of monthly mean modeled tropospheric columns with OMI observations

Maps of monthly mean tropospheric  $\text{NO}_2$  columns for all regional models as well as the global models are given in Figs. 3–6 for August and December 2008, as compared to OMI  $\text{NO}_2$  observations. The scale is approximately logarithmic and ranges over two orders of magnitude. In general all models capture well the observed main patterns of high and low  $\text{NO}_2$  columns over the densely populated regions, like the Benelux region

### Comparison of $\text{NO}_2$ in regional and global models to OMI

V. Huijnen et al.

Title Page

Abstract

Introduction

Conclusions

References

Tables

Figures

◀

▶

◀

▶

Back

Close

Full Screen / Esc

Printer-friendly Version

Interactive Discussion



and the large cities in Europe, and the low values over the Atlantic ocean. All regional models show more spatial variation in column data, because of the finer resolution, compared to the global models.

Whereas in summer OMI measures tropospheric NO<sub>2</sub> columns of more than 2×10<sup>15</sup> molec/cm<sup>2</sup> over a large part of continental Europe including the south-east region, the models only show high NO<sub>2</sub> over the populated west part of Europe. For instance, EURAD-IM, EMEP and BOLCHEM show tropospheric columns over 1×10<sup>15</sup> molec/cm<sup>2</sup> over Poland and Hungary, but the magnitude decreases on average below this level in east and south-east direction. This could indicate that the lifetime of NO<sub>2</sub> as it is advected is longer than predicted by most models. The lifetime is determined by NO<sub>x</sub> chemistry (including the conversion of reservoir species such as PAN), photolysis, dry and wet deposition. Only the SILAM model shows relatively large NO<sub>2</sub> columns all over the continent, indicating a longer NO<sub>2</sub> lifetime in this model. Only for Scandinavia and over the Atlantic Ocean low tropospheric columns are modeled.

On average the measured tropospheric NO<sub>2</sub> column increases in winter months, due to an increased NO<sub>2</sub> lifetime. In winter the average discrepancy between models and the retrieval, as was observed in summer time, has disappeared. However, regionally clear differences are observed. For instance, all models underestimate the very high NO<sub>2</sub> columns retrieved over the Po Valley. In December the difference between SILAM and the other RAQ models is smaller, although this model still shows relatively high columns.

The models do not capture the observed high concentrations at the African side of the Mediterranean as these emission sources are not included in the European TNO inventory. Ship tracks west and south from Spain can be observed from the OMI measurements. This is relatively well captured by TM5-Zoom, BOLCHEM, CAMx, MATCH, EMEP and SILAM. The TM5, MOZART-IFS, EURAD-IM, CHIMERE and CAC models show little evidence of enhanced NO<sub>2</sub> columns at the major shipping routes. The ship emissions have been omitted in EURAD-IM, CAC and in CHIMERE for the summer results, because they were not part of the TNO inventory. In the global models

## Comparison of NO<sub>2</sub> in regional and global models to OMI

V. Huijnen et al.

Title Page

Abstract

Introduction

Conclusions

References

Tables

Figures

⏪

⏩

◀

▶

Back

Close

Full Screen / Esc

Printer-friendly Version

Interactive Discussion



MOZART-IFS and TM5 the NO<sub>2</sub> is too diluted in the large grid-boxes to see any signal from shipping.

The EURAD-IM, EMEP and CAMx models show generally good correspondence to each other, and to the OMI-NO<sub>2</sub> product. BOLCHEM shows relatively high tropospheric columns over the big cities, and at the same time a similar low bias in rural areas as the other RAQ models. The MATCH model suffered from a relatively large low bias during the summer months, which has been identified as a problem in the application of the emission inventory. Also the MATCH model is in August relatively high at its domain boundaries over the Atlantic. From November onwards the overall low bias has disappeared, after a model-upgrade, where emissions are enhanced and boundary conditions are taken from MOZART-IFS. The CHIMERE model is well in line with other models for summer months, but misses the NO<sub>2</sub> hotspot over Madrid. This is attributed to a local implementation error for these emissions. Also tropospheric columns over Eastern Europe are significantly lower compared to the other models.

With respect to the global models, both in summer and winter MOZART-IFS shows low NO<sub>2</sub> columns compared to OMI, as well as most of the RAQ models. For instance, MOZART-IFS does not show the high columns over the western Europe region. The low bias in MOZART-IFS is attributed to the fact that NO<sub>x</sub> emission fluxes in this experiment have been under-represented by about a factor 2, which is resolved in a new model version. In the TM5 model on the 3×2° resolution the tropospheric NO<sub>2</sub> columns are on average higher than most of the RAQ models. This can be explained by the use of the RETRO emission inventory, which is significantly higher for this region than the TNO-inventory. The TM5 version with zoom region over Europe shows a much larger spatial detail in NO<sub>2</sub> columns, which results in a better spatial correlation with the observed columns. This is a consequence of the relatively short lifetime for NO<sub>2</sub>, combined with the availability of the GEMS-RETRO NO<sub>2</sub> emission inventory on a 0.5×0.5° resolution. On the other hand, the total columns in TM5-Zoom are also significantly higher compared to the reference run, and also compared to most of the other models. This illustrates that the use of high-resolution models is necessary to account

## Comparison of NO<sub>2</sub> in regional and global models to OMI

V. Huijnen et al.

Title Page

Abstract

Introduction

Conclusions

References

Tables

Figures

◀

▶

◀

▶

Back

Close

Full Screen / Esc

Printer-friendly Version

Interactive Discussion



for the spatial variation in NO<sub>2</sub>, but at the same time the applied parameterizations in the model, such as chemistry, photolysis and deposition, may cause differences in concentration fields as an effect of changing the model resolution.

Figure 7 shows the mean tropospheric NO<sub>2</sub> columns over the selected regions. In Table 4 the mean from all models and its spread, scaled to the model mean, are provided for winter (DJF) and summer (JJA) time periods. For the mid/south RAQ region the OMI measurements increase slightly from 1.9–2.8×10<sup>15</sup> molec/cm<sup>2</sup>. In summer months all models (except for SILAM) predict lower NO<sub>2</sub> columns than what is observed by OMI (the model average is 1.0×10<sup>15</sup> molec/cm<sup>2</sup> and the model spread is approximately 25% of the mean column). During winter months the model average is well in line with the observations; the model spread is of the size of 23% of the mean column. TM5-Zoom, SILAM, BOLCHEM and CHIMERE are positively biased in winter, most other models (except for CAMx and EURAD-IM) predict slightly lower columns compared to the OMI NO<sub>2</sub> measurements.

When looking at the West-European region the columns for both the models and the retrieval are on average higher than in the full domain. On average the model column is about 1.8 × 10<sup>15</sup> molec/cm<sup>2</sup> below the OMI NO<sub>2</sub> retrieval in summer, i.e. approximately 37%. For the Netherlands region the differences between the models increase even more, where BOLCHEM, SILAM, CHIMERE and TM5-Zoom are again relatively high.

In East-Europe the models show systematically lower NO<sub>2</sub> tropospheric columns in summer compared to OMI (except for SILAM), but they show a large increase in NO<sub>2</sub> in October. On the other hand, from January onwards most models over-predict NO<sub>2</sub> compared to OMI. It is remarkable that for this region OMI observations in June 2009 are significantly lower than in July 2008, which results in a good match of the models compared to OMI observations in Spring/Summer 2009. For North-Italy most RAQ models are below OMI in summer and autumn 2008, but show a better match from January onwards. Also for the Iberian Peninsula most models are below OMI with exceptions for SILAM, BOLCHEM and CHIMERE. As for East-Europe, OMI shows relatively low columns in spring 2009. Although the surface albedo maps in the DOMINO

## Comparison of NO<sub>2</sub> in regional and global models to OMI

V. Huijnen et al.

Title Page

Abstract

Introduction

Conclusions

References

Tables

Figures

◀

▶

◀

▶

Back

Close

Full Screen / Esc

Printer-friendly Version

Interactive Discussion



product have been replaced in winter 2009, a comparison of OMI observations for May-June 2008 to the 2009 data did not reveal a systematic trend for any of the regions. An under-estimation of  $\text{NO}_2$  in summertime in Southern Europe in the RAQ models can partially be explained by missing emission sources from biomass burning and lightning.

5 Also the application of the TNO emission inventory could explain an under-estimation in East and South-East Europe.

## 6 Comparison to in-situ observations in The Netherlands

The modeled monthly mean concentrations at the lowest model layer are compared to the Dutch Air Quality Monitoring Network (LML), (Beijk et al., 2007), at 13:00 UTC.

10 We have selected 17 rural stations as their measurements are considered most representative for the regions comparable to the coinciding the model grid (Blond et al., 2007). The corresponding model results have been interpolated in space and time to these measurement sites. The measurements of  $\text{NO}_2$  from the ground stations are all based on the chemiluminescence technique. It is well known that this method is

15 subject to interferences due to other  $\text{NO}_z$  components (e.g. PAN and  $\text{HNO}_3$ ), (Winer et al., 1974; Steinbacher et al., 2007). Here  $\text{NO}_z$  is defined as  $\text{NO}_y\text{-NO}_x$  with  $\text{NO}_y$  the sum of all reactive nitrogen oxides. This interference effect is stronger over background stations than in urban regions, larger in summer compared to winter, and larger in the afternoon than in the morning. A correction factor has been proposed by Lamsal et al.

20 (2008), based on the estimated ratio of  $\text{NO}_2$  to  $\text{NO}_z$ . This also accounts for the efficiency with which  $\text{NO}_z$  species are converted into NO on the molybdenum surface. Based on independent CHIMERE model results for  $\text{NO}_z$  (Boersma et al., 2009b), which have been validated for a rural measurement site at Taenikon (Lamsal et al., 2008), monthly-mean correction factors at 14:00 UTC for all individual stations have been calculated.

25 These factors range between 0.6 in summer (with a spread due to variations in the modeled concentrations of  $\sigma=0.14$ ), to 0.97 ( $\sigma=0.01$ ) in winter. This implies an increase of the seasonal cycle in the observations due to this interference correction.

### Comparison of $\text{NO}_2$ in regional and global models to OMI

V. Huijnen et al.

Title Page

Abstract

Introduction

Conclusions

References

Tables

Figures

◀

▶

◀

▶

Back

Close

Full Screen / Esc

Printer-friendly Version

Interactive Discussion



---

**Comparison of NO<sub>2</sub> in regional and global models to OMI**V. Huijnen et al.

---

[Title Page](#)[Abstract](#)[Introduction](#)[Conclusions](#)[References](#)[Tables](#)[Figures](#)[◀](#)[▶](#)[◀](#)[▶](#)[Back](#)[Close](#)[Full Screen / Esc](#)[Printer-friendly Version](#)[Interactive Discussion](#)

The comparison of the models to the corrected measurements is shown in Fig. 8. In summer 2008 the models are relatively close to the observations, on average 9% below the LML data for July–August 2008, see also Table 4. The modeled tropospheric columns are lower than OMI by 38%, which suggests that the OMI observations may be biased high for this region and period.

In DJF the models on average under-estimate the NO<sub>2</sub> concentrations by 24%. On the other hand tropospheric columns in this period are only low by 9%. This could suggest that those models with low surface concentration levels over-estimate boundary-layer mixing in this time period. On average the model spread in July–August is 33%, whereas in DJF this is 14%.

The MATCH and MOZART-IFS models predict the lowest surface concentrations, as in the evaluation of the tropospheric columns, whereas MATCH gets more in line with the other models from November onwards. In summer 2008 model data from TM5, EURAD-IM, EMEP and SILAM are well in line with observations. CAC is relatively low in summer 2008, but it is remarkable that this model, as well as SILAM, performs best in predicting the observed high concentrations in winter. EURAD-IM performs relatively well in Summer 2008 and winter, but has a negative bias in Spring 2009. TM5, TM5-Zoom, BOLCHEM, EMEP and CHIMERE show a relatively mild seasonal cycle, showing a good correspondence or over-estimation in spring/summer, and an under-estimation in winter. CAMx is both in summer and winter low. This all indicates that the individual model performance varies depending on the season, which supports the use of an ensemble of models for the prediction of surface concentrations.

## 7 Diurnal cycle

Figure 9 shows the diurnal cycle of the area-averaged tropospheric column for the region over The Netherlands. This region is chosen as it is well representative for regions with high anthropogenic emissions, which have a relatively large effect on the diurnal cycle for NO<sub>2</sub>. For this data no filtering for OMI-observations is applied. CAC

data and September data for SILAM was not available for this purpose. The models show significant differences in the diurnal cycle, and also higher values towards winter time compared to summer time, as was observed in the previous sections.

All models show a drop in NO<sub>2</sub> concentrations during daytime, related to the changing NO/NO<sub>2</sub> equilibrium, but the timing and magnitudes are different. At OMI overpass time (13:30 LT, which corresponds on average for this region to approximately 12:00 UTC) the models are close to their daytime minimum. The figures illustrate that in winter time the models are more sensitive to the timing of the sampling than in summer, as absolute differences between diurnal minima and maxima in the models are larger. Still, the ratio of the maximum over the minimum tropospheric column are allmost equal in winter compared to summer. For september this ratio is 1.65, with a spread in the models of 0.27, while in December this ratio is 1.55 (spread 0.24). Model results with GEOS-Chem over Israel (Boersma et al., 2009b), which also included a diurnal cycle in anthropogenic emissions, also showed a larger cycle in summer compared to winter. In their study larger ratios in summer were attributed to larger daytime NO<sub>2</sub> loss rates in summer compared to winter, due to increased photolysis. The numbers show that the variation between the models in magnitude of the diurnal cycle is of the order of 15%.

The RAQ models show a distinct peak in NO<sub>2</sub> concentrations in the evening, related to the rush hour emissions and the NO to NO<sub>2</sub> conversion. A modest peak in NO<sub>2</sub> is found also in the morning hours (06:00–09:00 UTC), which can also be attributed to increasing (traffic) emissions, before the photolysis rate of NO<sub>2</sub> is very efficient.

The global models capture the decrease in NO<sub>2</sub> during daytime, but to a lesser extend the increases in morning and evening hours, as predicted by the regional models. This can be attributed to the timing of emissions. In the global models these emissions are simply constant over the whole day, which results in an over-estimation of NO<sub>2</sub> concentrations during night-time and the reverse during daytime. The figures also show that NO<sub>2</sub> columns from TM5-Zoom for this region are higher over all day. BOLCHEM shows a remarkably strong diurnal cycle in summer. This could be related to the ap-

## Comparison of NO<sub>2</sub> in regional and global models to OMI

V. Huijnen et al.

Title Page

Abstract

Introduction

Conclusions

References

Tables

Figures

◀

▶

◀

▶

Back

Close

Full Screen / Esc

Printer-friendly Version

Interactive Discussion



plication of the relatively large fraction of NO<sub>2</sub> over NO, emitted into the model (15% of NO<sub>2</sub> versus 85% of NO), together with the increase in rush-hour emissions in the evening.

## 8 Effect of averaging kernel to the modeled total column

5 The tropospheric NO<sub>2</sub> retrieval algorithm accounts for the fact that the sensitivity of the satellite instrument is changing with altitude. On average OMI is more sensitive to NO<sub>2</sub> in the free troposphere than NO<sub>2</sub> in the boundary layer. This vertical sensitivity information is stored in the averaging kernel which depends on the satellite viewing geometry, and on aspects like the cloud cover and the surface reflectivity. This averaging kernel profile is included in the retrieval product (Boersma et al., 2009a). The retrieval of the vertical tropospheric column depends on independent information on the vertical distribution. In the case of OMI best-guess NO<sub>2</sub> tropospheric profiles have been derived from collocated TM4 model simulations sampled at local overpass time. This implies that the direct comparison of RAQ model tropospheric columns with the OMI product depends also on the quality of the TM4 simulations.

15 A better solution is the comparison between OMI and the modeled profile convoluted with the averaging kernel. In this case the actual satellite sensitivity profile is explicitly accounted for and the a priori TM4 profile shape no longer influences the comparison, (Eskes and Boersma, 2003). In mathematical language:  $(y - Ax)/y$  or  $(y - Ax)/Ax$  is independent of the a priori profile shape used in the retrieval, where  $y$  is the OMI observation,  $A$  is the averaging kernel, and  $x$  is the vertical profile of NO<sub>2</sub> partial columns of the model to be compared with OMI.

20 For most of the RAQ models only limited vertical information (concentration at a few vertical levels) was available for this study. For these models we have therefore compared the reported tropospheric NO<sub>2</sub> column with the OMI retrieval. Two models, EURAD-IM and CAMx, have provided the full 3-D model fields. We use these two models to answer the following questions:

### Comparison of NO<sub>2</sub> in regional and global models to OMI

V. Huijnen et al.

Title Page

Abstract

Introduction

Conclusions

References

Tables

Figures

◀

▶

◀

▶

Back

Close

Full Screen / Esc

Printer-friendly Version

Interactive Discussion



- (1) What is the quantitative difference between the column comparison and the comparison using the averaging kernel?
- (2) What is the error introduced by a missing upper troposphere in those models with a model top below the tropopause?
- 5 (3) What is the free troposphere contribution to the OMI tropospheric column observation?
- (4) How do the regional and global model profiles compare with the TM4 a priori profile?

Figure 10 shows the profiles for CAMx and EURAD-IM in terms of partial columns, compared to the TM4 a priori profiles. The TM4, CAMx and EURAD-IM fields are interpolated to the OMI observation locations. CAMx and EURAD-IM vertical levels are interpolated to the TM4 levels, on which also the kernel values are provided. The same surface and tropopause pressures are used in this interpolation. Also shown are the model profiles multiplied with the averaging kernel. This is a measure of the contribution of NO<sub>2</sub> from these levels to the total signal as measured by OMI. The integrated partial columns are denoted as  $N_{tc}$  for the total model column or  $N_k = Ax$  for the profile convoluted with the averaging kernel.

Table 5 lists the direct tropospheric columns over the western Europe region, as well as its contributions from the boundary layer (1000–800 hPa), the free troposphere, and also specifically the upper part of the free troposphere (500–200 hPa) as compared to the corresponding partial columns multiplied with the averaging kernels, for August and December 2008. The TM4 a priori column  $N_{tc}$  is identical to the convoluted column  $N_k$ , due to the definition of the averaging kernel. Surprisingly,  $N_{tc}$  and  $N_k$  for the CAMx and EURAD-IM models are very similar, both for August and December 2008.

The total, area-averaged columns with and without kernels for all months are shown in Fig. 11 as well as the corresponding average OMI retrieval. It shows that for other months the mean difference is small over the western Europe region. For other regions

## Comparison of NO<sub>2</sub> in regional and global models to OMI

V. Huijnen et al.

Title Page

Abstract

Introduction

Conclusions

References

Tables

Figures

◀

▶

◀

▶

Back

Close

Full Screen / Esc

Printer-friendly Version

Interactive Discussion



in Europe the observations are similar. Also the rms difference between  $N_k$  and  $N_{tc}$  is provided. This value does not exceed 10% in summer and approximately 20% in winter, which means that on average there is no significant cancellation of local differences between  $N_{tc}$  and  $N_k$ .

5 These results can be explained as follows. In the TM4/TM5 global model data a substantial (relative) contribution to the observed tropospheric column in summer can be attributed to  $\text{NO}_2$  in the free troposphere, which can be seen from the profiles of  $Ax_{TM4}$  in Fig. 10 and in Table 5 for the contribution of the free troposphere to  $N_k$  in TM4 and TM5. This contribution is much lower in the two RAQ models and also in the  
10 MOZART-IFS results. The MOZART-IFS system has much lower  $\text{NO}_2$  concentrations as compared to TM4/TM5, which can be attributed to slightly lower  $\text{NO}_2$  emissions in the free troposphere, and an under-representation of surface emissions. However, the FT/PBL ratio of the contributions to  $N_k$  is similar for the global models and larger than the regional models. The larger contribution to the free troposphere in TM4 than  
15 in MOZART-IFS could indicate a small potential (relative) under-estimation of the total tropospheric column in OMI. The difference between the EURAD-IM/CAMx partial columns and TM4/TM5 in the free troposphere in August is  $0.6 \times 10^{15}$  molec/cm<sup>2</sup> (approximately 10% of  $N_{tc}$ ), while when using the averaging kernel this difference increases to  $1.3\text{--}1.8 \times 10^{15}$  molec/cm<sup>2</sup> (approximately 25% of  $N_k$ ). The discrepancy between the RAQ models and the TM4/TM5 model versions could also be attributed to  
20 the missing aircraft emissions in the RAQ models as well as a missing parameterization for  $\text{NO}_x$  emissions due to lightning in EURAD-IM and CAMx. Most of the RAQ models are coupled to the global MOZART-IFS system, but this can only partly account for the missing  $\text{NO}_2$  sources by the influx through the boundaries.

25 Figure 10 shows that the TM4 a priori partial columns in the boundary layer are larger, and peaks at lower levels, compared to the RAQ models. This results into a relative over-estimation of OMI- $\text{NO}_2$  retrieval product. This is in line with Hains et al. (2009), who found that TM4 a priori partial columns in the boundary layer are higher compared to LIDAR measurements. Also Lamsal et al. (2009) showed that replacing

---

## Comparison of $\text{NO}_2$ in regional and global models to OMI

V. Huijnen et al.

---

[Title Page](#)[Abstract](#)[Introduction](#)[Conclusions](#)[References](#)[Tables](#)[Figures](#)[⏪](#)[⏩](#)[◀](#)[▶](#)[Back](#)[Close](#)[Full Screen / Esc](#)[Printer-friendly Version](#)[Interactive Discussion](#)

---

**Comparison of NO<sub>2</sub> in regional and global models to OMI**

---

V. Huijnen et al.

[Title Page](#)[Abstract](#)[Introduction](#)[Conclusions](#)[References](#)[Tables](#)[Figures](#)[⏪](#)[⏩](#)[◀](#)[▶](#)[Back](#)[Close](#)[Full Screen / Esc](#)[Printer-friendly Version](#)[Interactive Discussion](#)

the TM4 a priori profiles with GEOS-CHEM profiles, which have more mixed NO<sub>2</sub> concentrations in the boundary layer, leads to reduced tropospheric columns. Our current analysis of surface concentrations over the Netherlands support this conclusion. An analysis of the TM4 code as used in the DOMINO product revealed an implementation error for the NO<sub>2</sub> tracer field. Vertical transport including boundary layer mixing is applied on NO<sub>x</sub>, but not explicitly on NO<sub>2</sub>, right before sampling the NO<sub>2</sub> tracer field used in the retrieval algorithm.

The difference in the contribution from the boundary layer to  $N_{tc}$  between TM4 and the RAQ models is in summer-time about  $2.5 \times 10^{15}$  molec/cm<sup>2</sup>, i.e. the BL contribution to  $N_{tc}$  in TM4 is about 40% higher than in the EURAD-IM and CAMx models. The corresponding difference to  $N_k$  is  $1.7 \times 10^{15}$  molec/cm<sup>2</sup> (i.e. approximately 25% of  $N_k$ ). TM5 and TM5-Zoom is more alike to TM4. As the contributions from the boundary layer and the free troposphere are equal in magnitude, they partly compensate each other, which explains the similar numbers for  $N_k$  and  $N_{tc}$ , as observed from Fig. 11.

As suggested by Napelenok et al. (2008), also the contribution from the upper part of the free troposphere (higher than 500 hPa) may not be neglected. This is confirmed based on model results from the TM4 and TM5 models, see Table 5. In these models 5–10% of the tropospheric NO<sub>2</sub> column is situated at levels above 500 hPa in summer. Although emissions in the free troposphere are lower compared to the boundary layer, the NO<sub>2</sub> lifetime is much larger, due to lower temperatures. The percentual contribution in MOZART-IFS, CAMx and EURAD-IM at these levels is lower. The difference between TM5 and MOZART-IFS NO<sub>2</sub> concentrations in the upper part of the free troposphere can again be attributed to different aircraft and lightning emissions, as well as differences in the chemistry schemes. When considering the partial columns convoluted with the averaging kernels, the percentual contribution reaches a total of the order of 10–20% in the global models over the western Europe region, both in summer and in winter. Again, the CAMx and EURAD-IM models show a relatively small contribution, between 0 and 15% in summer and about 5% in winter, over this region. This implies that in the comparison of model output from regional models, convoluted

with averaging kernels, one has to correct for the contribution to the total column in the upper troposphere, if this region is not accounted for in the models.

From Fig. 10 and Table 5 it can be seen that in December the differences in the TM4-partial columns compared to CAMx and EURAD-IM are less significant, indicating less percentual difference when applying the averaging kernels to the observations. Also the mean OMI retrieval for this region shows that on average the discrepancy between the RAQ models and the OMI retrieval is high in summer, but decreases towards winter time, Fig. 11.

## 9 Model intercomparison of vertical profiles

The modeled total columns and surface observations are linked by the NO<sub>2</sub> profiles, Figs. 12 and 13. These figures show the monthly mean profiles at midday (12:00 UTC), using all available model data. The averaging is performed over the different regions, both for August and December 2008. The RAQ models have stored their output at four levels: the surface, 500, 1000 and 3000 m above the surface. These levels have been converted to pressure levels, using a standard surface pressure for the selected regions. For the global models as well as the RAQ models with full 3-D information (EURAD-IM/CAMx) the fields from all model levels are used.

The RAQ models show quantitatively similar mean profile shapes over the EU-RAQ domain. Only the SILAM model shows high NO<sub>2</sub> concentrations from the surface up to the free troposphere in the summer period. However, when zooming in to the highly polluted region over The Netherlands SILAM gets more in line with the other models. Most probably, there are several reasons for such behavior. Firstly, the model applies enhanced emissions over marine and some Eastern Europe regions. Secondly, the high background levels in monthly maps and vertical profiles over Eastern Europe suggest an extended NO<sub>2</sub> life time in comparison with the other RAQ models. In particular, the photolysis reaction of HNO<sub>3</sub> to NO<sub>2</sub> in SILAM could also lead to higher NO<sub>2</sub> concentrations. This feature is shared with, for example, TM5, which also tends to predict

## Comparison of NO<sub>2</sub> in regional and global models to OMI

V. Huijnen et al.

Title Page

Abstract

Introduction

Conclusions

References

Tables

Figures

◀

▶

◀

▶

Back

Close

Full Screen / Esc

Printer-friendly Version

Interactive Discussion



somewhat higher NO<sub>2</sub> background levels over Eastern Europe.

Apart from SILAM, the CHIMERE model concentrations are relatively high over the western Europe region, especially at about 900 hPa. Over Italy and specifically the Po-valley region the BOLCHEM and EMEP models show relatively large surface concentrations. Also over the Iberian Peninsula BOLCHEM shows relatively large concentrations at the surface. This was already identified in the analysis of the total columns. High concentration hotspots around the cities are found, whereas background concentrations match relatively well to OMI observations.

For the December data, similar features are observed as before. Only CAC is high, both in the boundary layer and the free troposphere, compared to the other RAQ models, which is in line with what was found in the comparison to surface observations.

With respect to the global models, the TM5 reference and TM5-Zoom models are well in line with the other RAQ models. The concentrations in the TM5-Zoom version are slightly larger than the reference run. In December the TM5 and TM5-Zoom are close together, and well in line with the other RAQ models. The concentrations from the MOZART-IFS system show a similar shape as the other RAQ models, but concentrations are lower both for July and December, even when averaged over the entire RAQ domain.

Differences in the profile shape in the models could partly be explained by the applied boundary layer mixing scheme. Models with enhanced mixing show lower NO<sub>2</sub> concentrations near the surface and a smaller vertical gradient in the boundary layer. Also the injection of NO<sub>x</sub> as either NO or NO<sub>2</sub> can influence NO<sub>2</sub> concentrations. BOLCHEM applies a distribution of 85% NO versus 15% NO<sub>2</sub> emissions, which is a relatively large amount of NO<sub>2</sub> injected in the model. In the other models the NO<sub>x</sub> emissions are introduced as at least 90% NO, up to 100% in the global models. This could lead to the high surface concentrations as observed locally over the Iberian Peninsula.

Other explanations are differences in the chemistry and photolysis scheme that determines the NO<sub>2</sub>/NO equilibrium. The photolysis rates are in turn affected by meteorology, as modeled cloud cover has an impact on the solar radiation. High NO<sub>2</sub> in

**Comparison of NO<sub>2</sub> in regional and global models to OMI**

V. Huijnen et al.

Title Page

Abstract

Introduction

Conclusions

References

Tables

Figures



Back

Close

Full Screen / Esc

Printer-friendly Version

Interactive Discussion



---

**Comparison of NO<sub>2</sub> in regional and global models to OMI**V. Huijnen et al.

---

[Title Page](#)[Abstract](#)[Introduction](#)[Conclusions](#)[References](#)[Tables](#)[Figures](#)[⏪](#)[⏩](#)[◀](#)[▶](#)[Back](#)[Close](#)[Full Screen / Esc](#)[Printer-friendly Version](#)[Interactive Discussion](#)

the free troposphere, as observed in SILAM, CHIMERE and BOLCHEM and in winter time the CAC model, could also be explained by the chemical mechanism. The conversion of NO<sub>2</sub> to other species depends on the OH concentration in the models: high OH concentrations lead to a reduced lifetime of NO<sub>x</sub>. However, the OH concentration and its variability depends on many other species, through the applied mechanism with different reaction rates. The presence of heterogeneous chemistry, and specifically the removal of N<sub>2</sub>O<sub>5</sub> by hydrolysis plays an important role in the removal of NO<sub>x</sub>, (Den-  
tener and Crutzen, 1993). Also acetone is important for the NO<sub>2</sub> chemistry. The original CBM-IV mechanism does not contain acetone as a separate trace gas. Therefore the PAN precursor CH<sub>3</sub>CO<sub>3</sub> is predominantly produced from CH<sub>3</sub>CHO+NO<sub>3</sub>, which is inefficient at low NO<sub>x</sub> concentrations. At low PAN concentrations significant variations between chemical mechanisms have been observed in an intercomparison study (Emmerson and Evans, 2009). As PAN is responsible for the transport of reactive nitrogen to cleaner regions of the atmosphere, this could indicate that models based on a CBM-IV formalism (CAMx, CAC, TM5) show relatively low NO<sub>2</sub> concentrations downwind from emission sources. On the other hand, in the modified CBM-IV scheme as applied in TM5, (Houweling et al., 1998), there appears no sign of a significant underestimation of PAN concentrations. Also organic nitrate can also transport significant amounts of NO<sub>2</sub> away from source regions (Williams et al., 2009).

## 10 Conclusions

We have presented a detailed intercomparison of tropospheric NO<sub>2</sub> from OMI measurements (the DOMINO product), a selection of RAQ models and two global models for a period of one year (July 2008–June 2009) over Europe. The models are all part of the GEMS forecast system. One of the global models (MOZART-IFS) is used to deliver boundary conditions to many of the RAQ models. For the other global model, TM5, a sensitivity study has been performed with increased resolution from 3×2° in the reference case to 1×1° over Europe for TM5-Zoom. The regional models apply very

similar anthropogenic emission inventories, but apart from that the models are characterized by considerable differences. The RETRO NO<sub>x</sub> emissions used in the global models is generally higher than the TNO emissions used in the RAQ models. We investigated the modeled NO<sub>2</sub> by attributing differences in the tropospheric columns to different altitude intervals and regions. For that reason the models have been compared both to OMI satellite observations and surface measurements, and additionally the model vertical NO<sub>2</sub> profile shapes have been intercompared.

Ideally the modeled tropospheric profiles should be convoluted with the averaging kernels, in order to cancel out the effect of the a priori profile shape in the averaging kernel, when comparing to the OMI NO<sub>2</sub> product. Based on results from two regional models (EURAD-IM and CAMx) and the global models, it was found that for area-averaged columns only a remarkably small bias is introduced by the neglect of the averaging kernel. The reason for this was that for the RAQ models in summer the higher sensitivity in the boundary layer happens to be largely compensated by the lower NO<sub>x</sub> in the free troposphere as compared to the TM4 a priori profile. In winter the profile shapes are more alike. The low NO<sub>2</sub> concentrations in the RAQ models compared to TM4 and TM5 in the free troposphere may be related to missing emissions from aircraft and lightning. These emissions are partly accounted for via the MOZART-IFS boundary conditions. However, MOZART-IFS concentrations of NO<sub>2</sub> in the free troposphere are also relatively low compared to TM4 and TM5. As a consequence also the RAQ models that use MOZART-IFS boundary conditions will have relatively low contribution of NO<sub>2</sub> due to these boundary conditions.

Validation studies (Hains et al., 2009; Lamsal et al., 2009; Zhou et al., 2009) have indicated a high-bias of OMI, especially in summer due to the a priori profile shape, the surface albedo map and the error in the air-mass factor at the surface. The combined effects lead to an estimated error of the order of 0–40% in summer. In winter-time the boundary layer concentrations as well as the concentrations in the free troposphere are more alike in the different models as compared to the OMI a priori profiles, which leads to a smaller total combined bias in the retrieval, of the order of 0–20%.

## Comparison of NO<sub>2</sub> in regional and global models to OMI

V. Huijnen et al.

[Title Page](#)[Abstract](#)[Introduction](#)[Conclusions](#)[References](#)[Tables](#)[Figures](#)[⏪](#)[⏩](#)[◀](#)[▶](#)[Back](#)[Close](#)[Full Screen / Esc](#)[Printer-friendly Version](#)[Interactive Discussion](#)

With these considerations in mind the remaining conclusions from this study can be summarized as follows:

- Good correspondence between models and surface observations over the Netherlands in summer, combined with the overall discrepancy between models and OMI over the western Europe region appear to confirm earlier findings, suggesting that OMI is biased high by approximately 40% in summer over polluted regions. We showed that the TM4 a priori  $\text{NO}_2$  concentrations near the surface as used in the retrieval algorithm are significantly larger relative to all contributing global and RAQ models. This is attributed to a missing vertical transport operation on  $\text{NO}_2$  (not on  $\text{NO}_x$ ) in this version of TM4.
- The upper part of the free troposphere (higher than 500 hPa) contributes up to about 10% of the tropospheric  $\text{NO}_2$  column, based on model results from the TM5 models over the Western Europe region in summer. For MOZART-IFS, EURAD-IM and CAMx this contribution is 0–5%. When considering the partial columns convoluted with the averaging kernels, the percentual contribution reaches up to 20%, both in summer and in winter. This implies that in the comparison of regional models convoluted with averaging kernels to OMI observations one has to correct for the contribution to the total column in the upper troposphere, in case that this region is not part of the model domain.
- By comparing the RAQ models to the OMI columns, a good correspondence of spatial patterns over Europe is observed, as well as their variation in magnitude. The global models capture substantially less detail. Also the seasonal cycle is captured by all models, but OMI shows a smaller amplitude of the seasonal cycle.
- On average for the middle and southern part of the RAQ-domain the mean of all models is in summer 45% below the OMI observations. The model spread is of the size of 25%. In winter both the mean of all models and the OMI  $\text{NO}_2$  are about  $2.8 \times 10^{15}$  molec/cm<sup>2</sup>, whereas the model spread is similar as in sum-

**Comparison of  $\text{NO}_2$  in regional and global models to OMI**

V. Huijnen et al.

Title Page

Abstract

Introduction

Conclusions

References

Tables

Figures



Back

Close

Full Screen / Esc

Printer-friendly Version

Interactive Discussion



**Comparison of NO<sub>2</sub> in regional and global models to OMI**

V. Huijnen et al.

Title Page

Abstract

Introduction

Conclusions

References

Tables

Figures



Back

Close

Full Screen / Esc

Printer-friendly Version

Interactive Discussion



mer. For regions with very high NO<sub>2</sub> concentrations, like over The Netherlands, the model spread is of the order of 20–40% both in summer and winter. Over The Netherlands the mean of all models is in summer 38% below the mean OMI observations, and in winter very close to OMI.

- The comparison of OMI observations to model data has revealed several missing emission sources in the models. The magnitude of the concentrations MOZART-IFS are low over the full EU-RAQ region, due to an under-representation of the surface fluxes in this model. This leads to low NO<sub>2</sub> concentrations in the free troposphere in the models that use MOZART-IFS as boundary conditions. Missing emission sources in the MATCH and CHIMERE have been resolved, as well as missing shipping emissions in EURAD-IM.
- In the SILAM model enhanced background concentrations in the free troposphere are observed, resulting in a better agreement with OMI in summer. The surface concentrations in The Netherlands are well in line with observations. This points at a significantly larger NO<sub>2</sub> residence time in SILAM, compared to the other models.
- Comparing TM5-Zoom to TM5 a better match to spatial variations was observed compared with OMI and the RAQ models. This illustrates that an improved resolution leads to a much better spatial correlation to OMI observations, due to the short lifetime and related strong concentration gradients for NO<sub>2</sub>. On the other hand the magnitude of the tropospheric columns is over-estimated in TM5-Zoom. This is attributed to larger NO<sub>2</sub> concentrations in boundary layer. It shows the resolution dependence of TM5 parameterizations (e.g. changing photolysis rates due to changing cloud cover information).
- Comparison to Dutch surface observations shows that on average the models perform better in summer than in winter, when concentrations are underpredicted. The seasonal cycle in surface observations is comparable or larger than given by the models, which suggests that the seasonal cycle in OMI is underestimated.

**Comparison of NO<sub>2</sub> in regional and global models to OMI**

V. Huijnen et al.

[Title Page](#)[Abstract](#)[Introduction](#)[Conclusions](#)[References](#)[Tables](#)[Figures](#)[⏪](#)[⏩](#)[◀](#)[▶](#)[Back](#)[Close](#)[Full Screen / Esc](#)[Printer-friendly Version](#)[Interactive Discussion](#)

The match of surface concentrations in summer confirms that the surface concentrations from the a priori OMI profile are over-estimated. In winter the total columns are reasonably in line with the OMI observations. This could suggest that vertical mixing in the models is too strong in winter, causing a reduction of modeled NO<sub>2</sub> at the surface.

- The diurnal ratio of maximum over minimum tropospheric columns are slightly larger in summer than in to winter, in line with a study by Boersma et al. (2009b). This is probably due to larger photolysis rates. The spread in the models in this ratio is of the order of 15% of the ratio itself.
- The profile shape for the different RAQ models are well comparable. They also correspond well to the profile shapes in the global models. The profiles themselves support the previously described analyses for the individual models.

It has been shown that the spread of the modeled NO<sub>2</sub> is of the order of 20–40%, depending on the season, region and height in the troposphere that is considered. This supports the use of an ensemble of models for the prediction of the regional air quality. It is acknowledged that only with the use of detailed information on the processes that rule NO<sub>2</sub>, such as emission, deposition, chemical reaction rates including photolysis and (vertical) transport, as well as the details from the implementation can lead to conclusive statements for each individual model contribution. This can only be achieved via dedicated sensitivity studies. The current analyses of models against OMI NO<sub>2</sub> observations have shown to be useful in the identification of model errors, such as the application of emissions, as well as in the quantification of uncertainties in the NO<sub>2</sub> retrieval product.

*Acknowledgements.* GEMS was funded by the European Commission under the EU Sixth Research Framework Programme, contract number SIP4-CT-2004-516099.

## References

- Acarreta, J., Haan, J. D., and Stammes, P.: Cloud pressure retrieval using the O<sub>2</sub>-O<sub>2</sub> absorption band at 477 nm, *J. Geophys. Res.*, 109, D05204, doi:10.1029/2003JD003915, 2004. 22281
- Andersson, C., Langner, J., and Bergström, R.: Interannual variation and trends in air pollution over Europe due to climate variability during 1958–2001 simulated with a regional CTM coupled to the ERA40 reanalysis, *Tellus B*, 59, 77–98, 2007. 22274, 22277, 22317
- Andersson-Sköld, Y. and Simpson, D.: Comparison of the chemical schemes of the EMEP MSC-W and the IVL photochemical trajectory models, *Atmos. Environ.*, 33, 1111–1129, 1999. 22317
- Beijk, R., Mooibroek, D., and Hoogerbrugge, R.: Air quality in the Netherlands, 2003–2006 (Jaaroverzicht luchtkwaliteit, in Dutch), RIVM report 680704002, RIVM report 680704002, Bilthoven, The Netherlands, 2007. 22277, 22288
- Bessagnet, B., Menut, L., Aymoz, G., Chepfer, H., and Vautard, R.: Modeling dust emissions and transport within Europe: the Ukraine March 2007 event, *J. Geophys. Res.*, 113, D15202, doi:10.1029/2007JD009541, 2008. 22274, 22277, 22317
- Blackadar, A.: High-resolution models of the planetary boundary layer, in: *Advances in Environmental Science and Engineering*, Vol. 1, edited by: Pfafflin, J. R. and Ziegler, E. N., Gordon and Breach, New York, 50–85, 1978. 22317
- Blond, N., Boersma, K., Eskes, H., van der A, R., van Roozendaal, M., Smedt, I. D., Bergametti, G., and Vautard, R.: Intercomparison of SCIAMACHY nitrogen dioxide observations, in situ measurements and air quality modeling results over Western Europe, *J. Geophys. Res.*, 112, D10311, doi:10.1029/2006JD007277, 2007. 22276, 22288
- Boersma, K. F., Eskes, H. J., and Brinksma, E.: Error analysis for tropospheric NO<sub>2</sub> retrieval from space, *J. Geophys. Res.*, 109, D04311, doi:10.1029/2003JD003962, 2004. 22282
- Boersma, K. F., Eskes, H. J., Veefkind, J. P., Brinksma, E. J., van der A, R. J., Sneep, M., van den Oord, G. H. J., Levelt, P. F., Stammes, P., Gleason, J. F., and Bucsela, E. J.: Near-real time retrieval of tropospheric NO<sub>2</sub> from OMI, *Atmos. Chem. Phys.*, 7, 2103–2118, 2007, <http://www.atmos-chem-phys.net/7/2103/2007/>. 22276, 22281, 22282
- Boersma, K. F., Jacob, D., Bucsela, E., Perring, A., Dirksen, R., van der A, R., Yantosca, R., Park, R., Wenig, M., Bertram, T., and Cohen, R.: Validation of OMI tropospheric NO<sub>2</sub> observations during INTEX-B and application to constrain NO<sub>x</sub> emissions over the eastern United States and Mexico, *Atmos. Environ.*, 42(19), 4480–4497, 2008. 22276, 22282

### Comparison of NO<sub>2</sub> in regional and global models to OMI

V. Huijnen et al.

Title Page

Abstract

Introduction

Conclusions

References

Tables

Figures

◀

▶

◀

▶

Back

Close

Full Screen / Esc

Printer-friendly Version

Interactive Discussion



- Boersma, K. F., Dirksen, R. J., Veefkind, J. P., Eskes, H. J., and van der A, R. J.: Dutch OMI NO<sub>2</sub> (DOMINO) data product, HE5 data file user manual, Tech. rep., KNMI, 2009a. 22281, 22282, 22291
- Boersma, K. F., Jacob, D. J., Trainic, M., Rudich, Y., DeSmedt, I., Dirksen, R., and Eskes, H. J.: Validation of urban NO<sub>2</sub> concentrations and their diurnal and seasonal variations observed from the SCIAMACHY and OMI sensors using in situ surface measurements in Israeli cities, *Atmos. Chem. Phys.*, 9, 3867–3879, 2009b, <http://www.atmos-chem-phys.net/9/3867/2009/>. 22276, 22282, 22288, 22290, 22301
- Bott, A.: A positive definite advection scheme obtained by nonlinear renormalization of the advective fluxes, *Mon. Weather Rev.*, 117, 1006–1015, 1989. 22317
- Bousserez, N., Attié, J.-L., Peuch, V.-H., Michou, M., Pfister, G., Edwards, D., Emmons, L., Mari, C., Barret, B., Arnold, S.R., Heckel, A., Richter, A., Schlager, H., Lewis, A., Avery, M., Sachse, G., Browell, E.V., and Hair, J.W.: Evaluation of the MOCAGE chemistry and transport model during the ICARTT/ITOP experiment, *J. Geophys. Res.*, 112, D10S45, doi:10.1029/2006JD00759, 2007. 22274, 22275
- Brinkma, E., Pinardi, G., Braak, R., Volten, H., Richter, A., Dirksen, R., Vlemmix, T., Swart, D., Knap, W., Veefkind, J., Eskes, H., Allaart, M., Rothe, R., Peters, A., and Levelt, P.: The 2005 and 2006 DANDELIONS NO<sub>2</sub> and Aerosol Intercomparison Campaigns, *J. Geophys. Res.*, 113, D16S46, doi:10.1029/2007JD008808, 2008. 22276, 22282
- Carter, W.: A detailed mechanism for the gas-phase atmospheric reactions of organic compounds, *Atmos. Environ.*, 24A, 481–518, 1990. 22278, 22317
- Carter, W.: Condensed atmospheric photooxidation mechanisms for isoprene, *Atmos. Environ.*, 30, 4275–4290, 1996. 22317
- Chen, J., Avise, J., Lamb, B., Salathé, E., Mass, C., Guenther, A., Wiedinmyer, C., Lamarque, J.-F., O'Neill, S., McKenzie, D., and Larkin, N.: The effects of global changes upon regional ozone pollution in the United States, *Atmos. Chem. Phys.*, 9, 1125–1141, 2009, <http://www.atmos-chem-phys.net/9/1125/2009/>. 22274
- Collela, P. and Woodward, P.: The piecewise parabolic method (PPM) for gas-dynamical simulations, *J. Comput. Phys.*, 54, 174–201, 1984. 22317
- Corbett, J. and Koehler, H.: Updated Emissions from Ocean Shipping, *J. Geophys. Res.*, 108(D20), 4650–4666, 2003. 22312
- Dentener, F. and Crutzen, P.: Reaction of N<sub>2</sub>O<sub>5</sub> on tropospheric aerosols: impact on the global distribution of NO<sub>x</sub>, O<sub>3</sub>, and OH, *J. Geophys. Res.*, 98, 7149–7163, 1993. 22297

---

## Comparison of NO<sub>2</sub> in regional and global models to OMI

V. Huijnen et al.

---

Title Page

Abstract

Introduction

Conclusions

References

Tables

Figures

◀

▶

◀

▶

Back

Close

Full Screen / Esc

Printer-friendly Version

Interactive Discussion



- Elbern, H., Strunk, A., Schmidt, H., and Talagrand, O.: Emission rate and chemical state estimation by 4-dimensional variational inversion, *Atmos. Chem. Phys.*, 7, 3749–3769, 2007, <http://www.atmos-chem-phys.net/7/3749/2007/>. 22274, 22277, 22317
- Emmerson, K. M. and Evans, M. J.: Comparison of tropospheric gas-phase chemistry schemes for use within global models, *Atmos. Chem. Phys.*, 9, 1831–1845, 2009, <http://www.atmos-chem-phys.net/9/1831/2009/>. 22297
- Endresen, Ø., Sørsgård, E., Sundet, J.K., Dalsøren, S.B., Isaksen, I.S.A., Berglen, T.F., and Gravir, G.: Emissions from international sea transport and environmental impact, *J. Geophys. Res.*, 108(D17), 4560, doi:10.1029/2002JD002898, 2003. 22312
- Eskes, H. J. and Boersma, K. F.: Averaging kernels for DOAS total-column satellite retrievals, *Atmos. Chem. Phys.*, 3, 1285–1291, 2003, <http://www.atmos-chem-phys.net/3/1285/2003/>. 22276, 22291
- Flemming, J., Inness, A., Flentje, H., Huijnen, V., Moinat, P., Schultz, M. G., and Stein, O.: Coupling global chemistry transport models to ECMWF's integrated forecast system, *Geosci. Model Dev. Discuss.*, 2, 763–795, 2009. 22275, 22278
- Galperin, M.: The approaches to correct computation of airborne pollution advection, in: *Problems of Ecological Monitoring and Ecosystem Modelling*, vol. XVII, *Gidrometeoizdat*, St. Petersburg, 54–68, 2000. 22317
- Geiger, H., Barnes, I., Bejan, I., Benter, T., and Spittler, M.: The tropospheric degradation of isoprene: an updated module for the regional atmospheric chemistry mechanism, *Atmos. Environ.*, 37, 1503–1519, 2003. 22317
- Gery, M. W., Whitten, G., Killus, J., and Dodge, M.: A photochemical kinetics mechanism for urban and regional scale computer modeling, *J. Geophys. Res.*, 94, 12925–12956, 1989. 22278, 22279, 22317
- Godowitch, J., Hogrefe, C., and Rao, S.: Diagnostic analysis of a regional air quality model: changes in modeled processes affecting ozone and chemical-transport indicators from NO<sub>x</sub> point source emission reductions, *J. Geophys. Res.*, 113, D19303, doi:10.1029/2007JD009537, 2008. 22274
- Gross, A., Amstrup, B., Baklanov, A., Lorenzen, T., and Sorensen, J.H.: CAC: An Air Pollution Model from Regional to Urban Scale Modelling, in: *COST-728/NetFAM Workshop on Integrated Systems of Meso-meteorological and Chemical Transport Models*, edited by: Baklanov, A., Mahura, A. and Sokhi, R., Copenhagen, 128–134, 2007. 22274, 22277, 22317
- Hains, J., Boersma, K., Kroon, M., Dirksen, R., Cohen, R., Perring, A., Bucsel, E., Volten, H.,

---

**Comparison of NO<sub>2</sub> in regional and global models to OMI**V. Huijnen et al.

---

[Title Page](#)[Abstract](#)[Introduction](#)[Conclusions](#)[References](#)[Tables](#)[Figures](#)[◀](#)[▶](#)[◀](#)[▶](#)[Back](#)[Close](#)[Full Screen / Esc](#)[Printer-friendly Version](#)[Interactive Discussion](#)

---

**Comparison of NO<sub>2</sub>  
in regional and global  
models to OMI**V. Huijnen et al.

---

[Title Page](#)[Abstract](#)[Introduction](#)[Conclusions](#)[References](#)[Tables](#)[Figures](#)[◀](#)[▶](#)[◀](#)[▶](#)[Back](#)[Close](#)[Full Screen / Esc](#)[Printer-friendly Version](#)[Interactive Discussion](#)

Swart, D., Richter, A., Wittrock, F., Schoenhardt, A., Wagner, T., Ibrahim, O., van Roozendaal, M., Pinardi, G., Gleason, J., Veefkind, P., and Levelt, P.: Testing and Improving OMI DOMINO Tropospheric NO<sub>2</sub> Using Observations from the DANDELIONS and INTEX-B Validation Campaigns, *J. Geophys. Res.*, doi:10.1029/2009JD012399, in review, 2009. 22282, 22283, 22293, 22298

Hollingsworth, A. R., Engelen, R. J., Textor, C., Benedetti, A., Boucher, O., Chevallier, F., De-  
thof, A., Elbern, H., Eskes, H., Flemming, J., Granier, C., Kaiser, J. W., Morcrette, J.-J.,  
Rayner, P., Peuch, V.-H., Rouil, L., Schultz, M. G., Simmons, A. J., and Consortium, T. G.: To-  
ward a monitoring and forecasting system for atmospheric composition: The GEMS project,  
*B. Am. Meteorol. Soc.*, 89, 1147–1164, 2008. 22274

Holtstlag, A. A. and Boville, B. A.: Local versus nonlocal boundary-layer diffusion in a global  
climate model, *J. Climate*, 10, 1825–1842, 1993. 22279, 22317

Holtstlag, A. A. and Moeng, C.-H.: Eddy diffusivity and counter-gradient transport in the convec-  
tive atmospheric boundary layer, *J. Atmos. Sci.*, 48, 1690–1698, 1991. 22317

Hong, S.-Y. and Pan, H.-L.: Nonlocal boundary layer vertical diffusion in a medium-range fore-  
cast model, *Mon. Weather Rev.*, 124, 2322–2339, 1996. 22317

Horowitz, L., Walters, S., Mauzerall, D., Emmons, L., Rasch, P., Granier, C., Tie, X., Lamar-  
que, J., Schultz, M., Tyndall, G., Orlando, J., and Brasseur, G.: A global simulation of  
tropospheric ozone and related tracers: description and evaluation of MOZART, version  
2, *J. Geophys. Res.*, 108(D24), 4784, doi:10.1029/2002JD002853, 2003. 22275, 22278,  
22312, 22317

Houweling, S., Dentener, F., and Lelieveld, J.: The impact of non-methane hydrocarbon com-  
pounds on tropospheric photochemistry, *J. Geophys. Res.*, 103, 10673–10696, 1998. 22279,  
22281, 22297, 22317

Huang, H.-C., Lin, J., Tao, Z., Choi, H., Patten, K., Kunkel, K., Xu, M., Zhu, J., Liang, X.-Z.,  
Williams, A., Caughey, M., Wuebbles, D. J., and Wang, J.: Impacts of long-range transport  
of global pollutants and precursor gases on US air quality under future climatic conditions,  
*J. Geophys. Res.*, 113, D19307, doi:10.1029/2007JD009469, 2008. 22274

Hubbard, M. and Nikiforakis, N.: A three-dimensional, adaptive, Godunov-type model for global  
atmospheric flows, *Mon. Weather Rev.*, 131, 1848–1864, 2003. 22317

Jones, A., Thomson, D., Hort, M., and Devenish, B.: The UK Met Office's Next-Generation  
Atmospheric Dispersion Model, NAME III, Springer, Berlin, 2007. 22274

Josse, B., Simon, P., and Peuch, V.-H.: Radon global simulations with the multiscale chemistry

- and transport model MOCAGE, *Tellus B*, 56-4, 339–356, 2004. 22274, 22275
- Kain, J.: The Kain-Fritsch convective parameterization: an update, *J. Appl. Meteorol.*, 43-1, 170–181, 2002. 22278
- Kinnison, D., Barsseur, G., Walters, S., Garcia, R., Marsh, D., Sassi, F., Harvey, V., Randall, C.,  
5 Emmons, L., Lamarque, J., Hess, P., Orlando, J., Tie, X., Randel, W., Pan, L., Gettelman, A.,  
Granier, C., Diehl, T., Niemeier, U., and Simmons, A.: Sensitivity of chemical tracers to  
meteorological parameters in the MOZART-3 chemical transport model, *J. Geophys. Res.*,  
112, D20302, doi:10.1029/2006JD007879, 2007. 22275, 22278, 22317
- Kleipool, Q. L., Dobber, M. R., de Haan, J. F., and Levelt, P. F.: Earth surface re-  
10 flectance climatology from 3 years of OMI data, *J. Geophys. Res.*, 113, D18308,  
doi:10.1029/2008JD010290, 2008. 22281, 22282
- Knowlton, K., Rosenthal, J., Hogrefe, C., Lynn, B., Gaffin, S., Goldberg, R., Rosenzweig, C.,  
Civerolo, K., Ku, J., and Kinney, P. L.: Assessing ozone-related health impacts under a chang-  
ing climate, *Environ. Health Persp.*, 112, 1557–1563, 2004. 22274
- 15 Köhler, I., Sausen, R., and Klenner, G.: NO<sub>x</sub> production from lightning. The impact of NO<sub>x</sub>  
emissions from aircraft upon the atmosphere at flight altitudes 8-15 km (AERONOX), Tech.  
rep., DLR, Obenpaffenhofen, Germany, 1995. 22280
- Krol, M., Houweling, S., Bregman, B., van den Broek, M., Segers, A., van Velthoven, P., Peters,  
W., Dentener, F., and Bergamaschi, P.: The two-way nested global chemistry-transport zoom  
20 model TM5: algorithm and applications, *Atmos. Chem. Phys.*, 5, 417–432, 2005,  
http://www.atmos-chem-phys.net/5/417/2005/. 22275, 22279, 22317
- Lamsal, L., Martin, R. V., van Donkelaar, A., Steinbacher, M., Celarier, E. A., Bucsela, E.,  
Dunlea, E. J., and Pinto, J. P.: Ground-level nitrogen dioxide concentrations inferred  
from the satellite-borne Ozone Monitoring Instrument, *J. Geophys. Res.*, 113, D16308,  
25 doi:10.1029/2007JD009235, 2008. 22288
- Lamsal, L., Martin, R. V., van Donkelaar, A., Celarier, E. A., Boersma, K. F., Dirksen, R., Luo, C.,  
and Wang, Y.: Indirect validation of tropospheric nitrogen dioxide retrieved from the OMI  
satellite instrument: insight into the seasonal variation of nitrogen oxides at northern midlati-  
tudes, *J. Geophys. Res.*, submitted, 2009. 22283, 22293, 22298
- 30 Lathi re, J., Hauglustaine, D., Noblet-Ducoudr , N. D., Krinner, G., and Folberth, G.: Past  
and future changes in biogenic volatile organic compound emissions simulated with a global  
dynamic vegetation model, *Geophys. Res. Lett.*, 32, L20818, doi:10.1029/2005GL024164,  
2005. 22312

---

**Comparison of NO<sub>2</sub>  
in regional and global  
models to OMI**V. Huijnen et al.

---

[Title Page](#)[Abstract](#)[Introduction](#)[Conclusions](#)[References](#)[Tables](#)[Figures](#)[◀](#)[▶](#)[◀](#)[▶](#)[Back](#)[Close](#)[Full Screen / Esc](#)[Printer-friendly Version](#)[Interactive Discussion](#)

- Lin, S. and Rood, R. B.: A fast flux form semi-Lagrangian transport scheme on the sphere, *Mon. Weather Rev.*, 124, 2046–2070, 1996. 22278, 22317
- Louis, J. F.: A parametric model of vertical eddy fluxes in the atmosphere, *Bound.-Lay. Meteorol.*, 17, 187–202, 1979. 22317
- 5 Markakakis, K., Im, U., Unal, A., Melas, D., Yenigun, O., and Incecik, S.: Compilation of a high resolution emissions inventory for the Greater Istanbul Area, *Sci. Total Environ.*, in review, 2009a. 22280
- Markakakis, K., Poupkou, A., Melas, D., Tzoumaka, P., and Petrakakis, M.: A computational approach based on GIS technology for the development of an anthropogenic emission inventory of gaseous pollutants in Greece, *Water Air Soil Poll.*, in press, doi:10.1007/s11270-009-0126-5, 2009b. 22280
- 10 Meijer, E., van Velthoven, P., Brunner, D., Huntrieser, H., and Kelder, H.: Improvement and evaluation for the parametrisation of nitrogen oxide production by lightning, *Phys. Chem. Earth*, 26(8), 557–583, 2001. 22312
- 15 Mircea, M., D’Isidoro, M., Maurizi, A., Vitali, L., Monforti, F., Zanini, G., and Tampieri, F.: A comprehensive performance evaluation of the air quality model BOLCHEM to reproduce the ozone concentrations over Italy, *Atmos. Environ.*, 42(6), 1169–1185, 2008. 22274, 22277, 22317
- Morris, R., Lau, S., and Yarwood, G.: Development and Application of an Advanced Air Toxics Hybrid Photochemical Grid Modeling System, Presented at 96th Annual Conference and Exhibition of the A&WMA, San Diego, California, 2003. 22274, 22277, 22317
- 20 Napelenok, S. L., Pinder, R. W., Gilliland, A. B., and Martin, R. V.: A method for evaluating spatially-resolved NO<sub>x</sub> emissions using Kalman filter inversion, direct sensitivities, and space-based NO<sub>2</sub> observations, *Atmos. Chem. Phys.*, 8, 5603–5614, 2008, <http://www.atmos-chem-phys.net/8/5603/2008/>. 22276, 22294
- 25 Nolte, C., Gilliland, A., Hogrefe, C., and Mickley, L.: Linking global to regional models to assess future climate impacts on surface ozone levels in the United States, *J. Geophys. Res.*, 113, D14307, doi:10.1029/2007JD008497, 2008. 22274
- Ohara, T., Akimoto, H., Kurokawa, J., Horii, N., Yamaji, K., Yan, X., and Hayasaka, T.: An Asian emission inventory of anthropogenic emission sources for the period 1980–2020, *Atmos. Chem. Phys.*, 7, 4419–4444, 2007, <http://www.atmos-chem-phys.net/7/4419/2007/>. 22312
- 30 Pleim, J. and Chang, J.: A non-local closure model for vertical mixing in the convective bound-

---

## Comparison of NO<sub>2</sub> in regional and global models to OMI

V. Huijnen et al.

---

Title Page

Abstract

Introduction

Conclusions

References

Tables

Figures

◀

▶

◀

▶

Back

Close

Full Screen / Esc

Printer-friendly Version

Interactive Discussion



- ary layer, *Atmos. Environ.*, 26A, 965–981, 1992. 22317
- Price, C., Penner, J., and Prather, M.: NO<sub>x</sub> from lightning 1. Global distribution based on lightning physics, *J. Geophys. Res.*, 102(D5), 5929–5941, 1997. 22312
- Randerson, J., van der Werf, G. R., Collatz, G. J., Giglio, L., Still, C. J., Kasibhatla, P., Miller, J. B., White, J. W. C., DeFries, R. S., and Kasischke, E. S.: Fire emissions from C<sub>3</sub> and C<sub>4</sub> vegetation and their influence on interannual variability of atmospheric CO<sub>2</sub> and δ<sup>13</sup>CO<sub>2</sub>, *Global Biogeochem. Cy.*, 19, GB2019, doi:10.1029/2004GB002366, 2005. 22312
- Robertson, L., Langner, J., and Engardt, M.: An Eulerian limited-area atmospheric transport model, *J. Appl. Meteorol.*, 38, 190–210, 1999. 22317
- Rouil, L., Honoré, C., Vautard, R., Beekmann, M., Bessagnet, B., Malherbe, L., Meleux, F., Dufour, A., Elichegaray, C., Flaud, J.-M., Menut, L., Martin, D., Peuch, A., Peuch, V.-H., and Poisson, N.: Prevair: an operational forecasting and mapping system for air quality in Europe, *B. Am. Meteorol. Soc.*, 90, 73–83, 2009. 22274
- Russell, G. L. and Lerner, J. A.: A new finite-differencing scheme for the tracer transport equation, *J. Appl. Meteorol.*, 20, 1483–1498, 1981. 22279, 22317
- Sander, S., Friedl, R., Ravishankara, A., Golden, D., Kolb, C., Kurylo, M., Molina, M., Moortgart, G., Keller-Rudek, H., Finlayson-Pitts, B., Wine, P., Huie, R., and Orkin, V.: Chemical Kinetics and Photochemical Data for Use in Atmospheric studies, Evaluation No. 15, Tech. rep., JPL, 2006. 22279
- Schaub, D., Boersma, K. F., Kaiser, J. W., Weiss, A. K., Folini, D., Eskes, H. J., and Buchmann, B.: Comparison of GOME tropospheric NO<sub>2</sub> columns with NO<sub>2</sub> profiles deduced from ground-based in situ measurements, *Atmos. Chem. Phys.*, 6, 3211–3229, 2006, <http://www.atmos-chem-phys.net/6/3211/2006/>. 22282
- Schmidt, H., Derognat, C., Vautard, R., and Beekmann, M.: A comparison of simulated and observed ozone mixing ratios for the summer of 1998 in Western Europe, *Atmos. Environ.*, 35, 6277–6297, 2001. 22278, 22317
- Schumann, U. (Ed.): Pollution from Aircraft Emissions in the North Atlantic Flight Corridor (POLINAT), Rep. 58, EUR 16978 EN, Brussels, 1997. 22312
- Simpson, D., Andersson-Sköld, Y., and Jenkin, M.: Updating the chemical scheme for the EMEP MSC-W oxidant model: Current status, EMEP MSC-W Note 2/93, 1993. 22278, 22317
- Simpson, D., Fagerli, H., Jonson, J., Tsyro, S., Wind, P., and Tuovinen, J.-P.: Transboundary acidification and eutrophication and ground level ozone in Europe: Unified EMEP Model

---

**Comparison of NO<sub>2</sub> in regional and global models to OMI**V. Huijnen et al.

---

[Title Page](#)[Abstract](#)[Introduction](#)[Conclusions](#)[References](#)[Tables](#)[Figures](#)[◀](#)[▶](#)[◀](#)[▶](#)[Back](#)[Close](#)[Full Screen / Esc](#)[Printer-friendly Version](#)[Interactive Discussion](#)

---

**Comparison of NO<sub>2</sub>  
in regional and global  
models to OMI**V. Huijnen et al.

---

[Title Page](#)[Abstract](#)[Introduction](#)[Conclusions](#)[References](#)[Tables](#)[Figures](#)[◀](#)[▶](#)[◀](#)[▶](#)[Back](#)[Close](#)[Full Screen / Esc](#)[Printer-friendly Version](#)[Interactive Discussion](#)

Description, EMEP/MSC-W Report EMEP Status Report 1/2003 Part I, The Norwegian Meteorological Institute, Oslo, Norway, 2003. 22274, 22277, 22317

Smagorinsky, J.: General circulation experiments with the primitive equations, *Mon. Weather Rev.*, 91, 99–164, 1963. 22317

5 Smolarkiewicz, P. K.: A simple positive definite advection scheme with small implicit diffusion, *Mon. Weather Rev.*, 111, 1968–1983, 1983. 22317

Society, E. I.: Generation of European Emission Data for Episodes (GENEMIS) project, Eurotrac annual report 1993, part 5, technical report, EUROTRAC, Garmish-Partenkirchen, Germany, 1994. 22280

10 Sofiev, M.: A model for the evaluation of long-term airborne pollution transport at regional and continental scales, *Atmos. Environ.*, 34(15), 2481–2493, 2000. 22317

Sofiev, M.: Extended resistance analogy for construction of the vertical diffusion scheme for dispersion models, *J. Geophys. Res.*, 107(D12), 2481–2493, 2002. 22317

Sofiev, M., Galperin, M., and Genikhovich, E.: Construction and evaluation of Eulerian dynamic core for the air quality and emergency modeling system SILAM, in: NATO Science for Peace and Security Series C: Environmental Security. Air pollution modelling and its application, XIX, edited by: Borrego, C. and Miranda, A., Springer, Netherlands, 699–701, 2008a. 22274, 22277, 22317

20 Sofiev, M., Siljamo, P., Karppinen, A., and Kukkonen, J.: Air quality forecasting during summer 2006: forest fires as one of major pollution sources in Europe, in: NATO Science for Peace and Security Series C: Environmental Security. Air pollution modelling and its application, XIX, edited by: Borrego, C. and Miranda, A., Springer, Netherlands, 305–312, 2008b. 22317

Steinbacher, M., Zellweger, C., Schwarzenbach, B., Bugmann, S., Buchmann, B., Ordóñez, C., Prevot, A. S. H., and Hueglin, C.: Nitrogen oxides measurements at rural sites in Switzerland: bias of conventional measurement techniques, *J. Geophys. Res.*, 112, D11307, doi:10.1029/2006JD007971, 2007. 22288

Stockwell, W., Kirchner, F., Kuhn, M., and Seefeld, S.: A new mechanism for regional atmospheric chemistry modeling, *J. Geophys. Res.*, 102, 25847–25879, 1997. 22317

30 Tarrasón, L., Benedictow, A., Fagerli, H., Jonson, J.E., Klein, H., van Loon, M., Simpson, D., Tsyro, S., Vestreng, V., Wind, P., Forster, C., Stohl, A., Amann, M., Cofala, J., Langner, J., Andersson, A. and Bergström, R.: Transboundary acidification and eutrophication and ground level ozone in Europe in 2003, Joint MSC-W & CCC & CIAM Report EMEP Status Report 1/2005, The Norwegian Meteorological Institute, Oslo, Norway, 2005. 22279, 22280

- Undén, P., Rontu, L., Järvinen, H., Lynch, P., Calvo, J., Cats, G., Cuxart, J., Eerola, K., Fortelius, C., Garcia-Moya, J. A., Jones, C., Lenderlink, G., McDonald, A., McGrath, R., Navascues, B., Nielsen, N. W., Ødegaard, V., Rodriguez, E., Rummukainen, M., Rõõm, R., Sattler, K., Sass, B. H., Savijärvi, H., Schreuer, B. W., Sigg, R., The, H., and Tijm, A.: HIRLAM-5 Scientific Documentation, Hirlam Scientific Report, 2002. 22317
- van Leer, B.: Towards the ultimate conservative difference scheme. V. A second-order sequel to Godunov's method., *J. Comp. Phys.*, 32, 101–136, 1979. 22317
- van Noije, T. P. C., Eskes, H. J., Dentener, F. J., Stevenson, D. S., Ellingsen, K., Schultz, M. G., Wild, O., Amann, M., Atherton, C. S., Bergmann, D. J., Bey, I., Boersma, K. F., Butler, T., Cofala, J., Drevet, J., Fiore, A. M., Gauss, M., Hauglustaine, D. A., Horowitz, L. W., Isaksen, I. S. A., Krol, M. C., Lamarque, J.-F., Lawrence, M. G., Martin, R. V., Montanaro, V., Müller, J.-F., Pitari, G., Prather, M. J., Pyle, J. A., Richter, A., Rodriguez, J. M., Savage, N. H., Strahan, S. E., Sudo, K., Szopa, S., and van Roozendaal, M.: Multi-model ensemble simulations of tropospheric NO<sub>2</sub> compared with GOME retrievals for the year 2000, *Atmos. Chem. Phys.*, 6, 2943–2979, 2006, <http://www.atmos-chem-phys.net/6/2943/2006/>. 22275
- Vestreng, V.: Review and revision. Emission data reported to CLRTP, Technical report, EMEP MSC-W, Norwegian Meteorological Institute, Oslo, Norway 2003. 22280, 22312
- Visschedijk, A. and van der Gon, H. D.: Gridded European Anthropogenic Emission Data for NO<sub>x</sub>, SO<sub>2</sub>, NMVOC, NH<sub>3</sub>, CO, PM<sub>10</sub>, PM<sub>2.5</sub> and CH<sub>4</sub> for the Year 2000, Technical Report TNO B&O-A Rapport 2005/106, 2nd version, TNO, Apeldoorn, 2005. 22279, 22312
- Visschedijk, A., Zandveld, P., and van der Gon, H. D.: A High Resolution Gridded European Emission Database for the EU Integrated Project GEMS, Technical Report TNO-report 2007-A-R0233/B, TNO, Apeldoorn, 2007. 22279, 22312
- Wagner, A., Adams, M., and Gugele, B.: ETC-ACC Air Emissions Spreadsheet for Belgrade Report (Emissions 1990–2003), Based On the Gap-Filled Air Emission Spreadsheet Delivered Under the 2005 ETC-ACC Subvention, Tech. rep., European Topic Centre on Air and Climate Change, 2005. 22279
- Williams, J. and van Noije, T.: On the Upgrading of the Modified Carbon Bond Mechanism IV for Use in Global Chemistry Transport Models, Scientific Report WR-2008-02, KNMI, De Bilt, The Netherlands, 2008. 22279, 22317
- Williams, J. E., Scheele, M. P., van Velthoven, P. F. J., Cammas, J.-P., Thouret, V., Galy-Lacaux, C., and Volz-Thomas, A.: The influence of biogenic emissions from Africa on tropical tropo-

---

**Comparison of NO<sub>2</sub> in regional and global models to OMI**V. Huijnen et al.

---

[Title Page](#)[Abstract](#)[Introduction](#)[Conclusions](#)[References](#)[Tables](#)[Figures](#)[◀](#)[▶](#)[◀](#)[▶](#)[Back](#)[Close](#)[Full Screen / Esc](#)[Printer-friendly Version](#)[Interactive Discussion](#)

spheric ozone during 2006: a global modeling study, Atmos. Chem. Phys., 9, 5729–5749, 2009,

<http://www.atmos-chem-phys.net/9/5729/2009/>. 22297

5 Winer, A., Peters, J. W., Smith, J. P., and Pitts Jr., J. N.: Response of commercial chemiluminescent NO-NO<sub>2</sub> analyzers to other nitrogen containing compounds, Environ. Sci. Technol., 8, 1118–1121, 1974. 22288

Yang, X., Kmit, M., Petersen, C., Nielsen, N. W., Sass, B. H., and Amstrup, B.: The DMI-HIRLAM Upgrade in November 2005, DMI Technical Report 05-15, Danish Meteorological Institute, online available at: <http://www.dmi.dk/dmi/tr05-15.pdf>, 2005. 22317

10 Zhou, Y., Brunner, D., Boersma, K. F., Dirksen, R., and Wang, P.: An improved tropospheric NO<sub>2</sub> retrieval for OMI observations in the vicinity of mountainous terrain, Atmos. Meas. Tech., 2, 401–416, 2009,

<http://www.atmos-meas-tech.net/2/401/2009/>. 22283, 22298

---

**Comparison of NO<sub>2</sub>  
in regional and global  
models to OMI**

V. Huijnen et al.

---

Title Page

Abstract

Introduction

Conclusions

References

Tables

Figures

◀

▶

◀

▶

Back

Close

Full Screen / Esc

Printer-friendly Version

Interactive Discussion



## Comparison of NO<sub>2</sub> in regional and global models to OMI

V. Huijnen et al.

**Table 1.** Specification of NO<sub>x</sub> emission inventories, in terms of Tg N/yr.

Models	Emission type (inventory)	Global (Tg N/yr)	EU-RAQ region (Tg N/yr)
MOZART-IFS	RETRO	23.9	4.6
	AMVER-V1 ships (Endresen et al., 2003)	3.5	0.3
	GFED-v2 10 year av. (Randerson et al., 2005)	5.6	0.05
	Biogenic (Lathière et al., 2005)	9.3	0.6
	Aircraft (Horowitz et al., 2003)	0.7	0.1
	lightning (Price et al., 1997)	4.0	0.09
TM5	RETRO/REAS (Ohara et al., 2007)	25.7	4.6
	Ships (Corbett and Koehler, 2003)	6.3	0.6
	GFED v2 5 year av. (Randerson et al., 2005)	5.4	0.05
	Biogenic (Lathière et al., 2005)	9.3	0.6
	Aircraft (Schumann et al., 1997)	0.7	0.1
	lightning (Meijer et al., 2001)	5.8	0.15
RAQ models	TNO anthropog. (Visschedijk et al., 2007; Visschedijk and van der Gon, 2005)	–	4.2
	EMEP shipping (Vestrenq, 2003)	–	0.2

Title Page

Abstract

Introduction

Conclusions

References

Tables

Figures

◀

▶

◀

▶

Back

Close

Full Screen / Esc

Printer-friendly Version

Interactive Discussion



**Comparison of NO<sub>2</sub>  
in regional and global  
models to OMI**

V. Huijnen et al.

**Table 2.** Definition of regions.

Region	Lon.	Lat.
EU-RAQ	–15–35	35–70
Mid/south RAQ	–15–35	35–57
Western Europe	–3–10	48–54
Eastern Europe	10–30	47–54
Italy	7–16	40–47
Iberian Peninsula	–10–2	36–44.5
The Netherlands	4.3–6.6	51–53.3

[Title Page](#)[Abstract](#)[Introduction](#)[Conclusions](#)[References](#)[Tables](#)[Figures](#)[⏪](#)[⏩](#)[◀](#)[▶](#)[Back](#)[Close](#)[Full Screen / Esc](#)[Printer-friendly Version](#)[Interactive Discussion](#)

## Comparison of NO<sub>2</sub> in regional and global models to OMI

V. Huijnen et al.

**Table 3.** Applied strategy for data stratification.

Data type	Regional stratification	Temporal stratification
Total columns	All regions	Interpolated at 13:30 LT; when OMI obs. available
Surface concentrations	NL region	12:00 UTC (13:00 LT); when surf. obs. available
Diurnal cycle	NL region	All data on hourly basis
Profiles	All regions	12:00 UTC; all model data

Title Page

Abstract

Introduction

Conclusions

References

Tables

Figures

◀

▶

◀

▶

Back

Close

Full Screen / Esc

Printer-friendly Version

Interactive Discussion



## Comparison of NO<sub>2</sub> in regional and global models to OMI

V. Huijinen et al.

**Table 4.** Regional mean of all models, and in brackets their ratios to OMI observations, for DJF and JJA. Also the model spread is given as percentage to OMI observations. In the bottom line the mean (and spread) surface concentrations of all models is provided, and their ratios compared to LML observations for DJF and JA.

Region	Mean [ $10^{15}$ molec/cm <sup>2</sup> ]		Spread	
	DJF (ratio, [%])	JJA (ratio, [%])	DJF ratio, [%]	JJA ratio, [%]
Mid/south RAQ	2.8 (96)	1.0 (54)	23	25
Western Europe	7.4 (84)	3.1 (63)	18	29
Eastern Europe	4.0 (101)	1.1 (50)	30	29
Italy	3.8 (79)	1.2 (65)	19	41
Iberian Pen.	2.4 (69)	1.2 (71)	19	37
Netherlands	9.4 (91)	4.6 (62)	21	29
LML [ppb]	9.9 (76)	2.9 (91)	14	33

Title Page

Abstract

Introduction

Conclusions

References

Tables

Figures

◀

▶

◀

▶

Back

Close

Full Screen / Esc

Printer-friendly Version

Interactive Discussion



## Comparison of NO<sub>2</sub> in regional and global models to OMI

V. Huijinen et al.

**Table 5.** Total tropospheric columns over West-Europe with/without kernel. In brackets the contribution from the boundary layer (1000–800 hPa), the free troposphere (800–200 hPa) and the upper part of the free troposphere (500–200 hPa). Note that  $N_k$  from TM4 is identical to the OMI retrieval product. Data shown for August and December.

Model	August		December	
	$N_{tc}$	$N_k$	$N_{tc}$	$N_k$
TM4	5.8 (4.8/1.0/0.4)	5.8 (3.6/2.2/1.0)	9.3 (8.7/0.6/0.1)	9.3 (6.9/2.4/0.9)
EURAD-IM	2.7 (2.3/0.4/0.1)	2.8 (1.9/0.9/0.4)	7.8 (7.3/0.5/0.1)	7.6 (5.7/1.9/0.5)
CAMx	2.6 (2.3/0.3/0.0)	2.3 (1.8/0.5/0.0)	9.4 (8.9/0.5/0.0)	9.5 (7.9/1.5/0.2)
TM5	4.0 (3.1/0.8/0.5)	5.1 (2.2/2.3/1.6)	7.8 (7.2/0.6/0.3)	8.6 (5.8/2.9/1.6)
TM5-Zoom	5.3 (4.5/0.8/0.3)	5.4 (3.3/2.1/1.2)	10.8 (10.1/0.7/0.3)	11.1 (7.8/3.1/1.7)
MOZART-IFS	1.9 (1.6/0.3/0.1)	2.1 (1.2/0.9/0.4)	6.4 (6.0/0.4/0.1)	6.3 (4.8/1.5/0.5)

Title Page

Abstract

Introduction

Conclusions

References

Tables

Figures

◀

▶

◀

▶

Back

Close

Full Screen / Esc

Printer-friendly Version

Interactive Discussion



## Comparison of NO<sub>2</sub> in regional and global models to OMI

V. Huijnen et al.

**Table 6.** Specifications of the global and regional CTM's.

	Institute, contact author	Resolution (lon/lat) n. lev., top lev.	Meteorology	Chemistry	Advection	Diffusion
BOLCHEM Mircea et al. (2008)	ISAC-CNR, A. Maurizi, M. D'Isidoro	0.4×0.4, L16, 500 hPa	BOLAM/ECMWF	SAPRC-90 Carter (1990)	WAF, Hubbard and Nikiforakis (2003)	–
CAC Gross et al. (2007)	DMI A. Gross	0.2×0.2, L25, 250 hPa	DMI-HIRLAM Undén et al. (2002) Yang et al. (2005)	CBM-IV+updates Gery et al. (1989); Carter (1996)	Bott (1989)	Smagorinsky (1963)
CHIMERE Bessagnet et al. (2008)	INERIS/LISA/LMD G. Foret	0.5×0.5	3hr ECMWF	MELCHIOR II Schmidt et al. (2001)	Collela and Woodward (1984) van Leer (1979)	Louis (1979)
EMEP-CWF <sup>b</sup> Simpson et al. (2003)	met.no, A. Valdebenito	0.25×0.25, L20, 100 hPa	3hr ECMWF	EMEP-MS-CW Andersson-Sköld and Simpson (1999) Simpson et al. (1993)	Bott (1989)	Louis (1979) K-theory
EURAD-IM Elbern et al. (2007)	RIU H. Elbern	0.4×0.4 <sup>a</sup> , L23, 100 hPa	MM5	RACM Stockwell et al. (1997) updated isoprene Geiger et al. (2003)	Bott (1989), Smolarkiewicz (1983)	Blackadar (1978) Pleim and Chang (1992)
MATCH Andersson et al. (2007)	SMHI L. Robertson	0.2×0.2, L30, 400 hPa	6hr ECMWF	EMEP, Simpson et al. (1993)	Bott (1989), Robertson et al. (1999)	Holtstlag and Moeng (1991), none above BL.
CAMx Morris et al. (2003)	NKUA, I. Kioutsioukis, A. Poupkou	0.3×0.3, L15, 300 hPa	MM5/ECMWF	CBM-IV + updates Gery et al. (1989), Carter (1996)	Collela and Woodward (1984)	K-theory, coeff. from MM5 Hong and Pan (1996)
MOZART-IFS Horowitz et al. (2003), Kinnison et al. (2007)	MPI/ECMWF, O. Stein/J. Flemming	1.9×1.9, L60, 0.1 hPa	1hr ECMWF	Kinnison et al. (2007)	Lin and Rood (1996)	Holtstlag and Boville (1993)
SILAM Sofiev et al. (2008a,b)	FMI M. Sofiev	0.2×0.2, L9, 200hPa	3hr ECMWF	Own development, NO <sub>x</sub> resembles Sofiev (2000)	Galperin (2000)	Sofiev (2002)
TM5 Krol et al. (2005)	KNMI V. Huijnen	3.0×2.0, L34, 0.1 hPa	3hr ECMWF	updated CBM-IV Gery et al. (1989), Houweling et al. (1998), Williams et al. (2008)	Russell and Lerner (1981)	Holtstlag and Boville (1993)

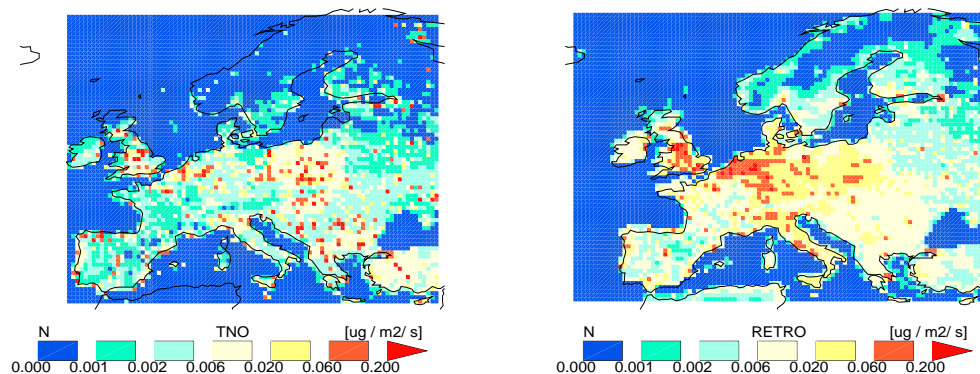
<sup>a</sup> EURAD-IM applies a 0.15×0.125 resolution after 13 February 2009.

<sup>b</sup> For EMEP the forecast version of the Unified EMEP model is used, denoted as EMEP-CWF.

[Title Page](#)
[Abstract](#)
[Introduction](#)
[Conclusions](#)
[References](#)
[Tables](#)
[Figures](#)
[Back](#)
[Close](#)
[Full Screen / Esc](#)
[Printer-friendly Version](#)
[Interactive Discussion](#)


## Comparison of NO<sub>2</sub> in regional and global models to OMI

V. Huijnen et al.

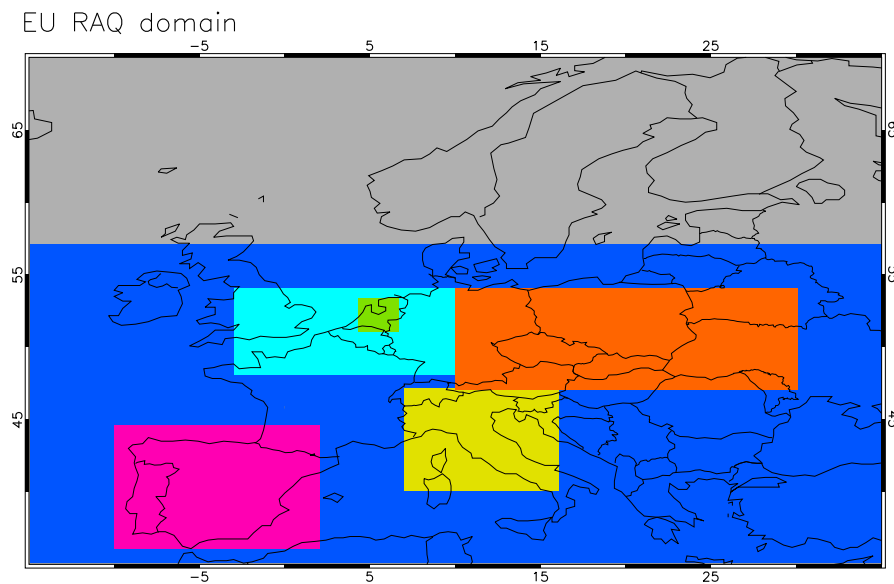


**Fig. 1.** TNO and RETRO anthropogenic NO<sub>x</sub> emissions in terms of  $\mu\text{g N/m}^2/\text{s}$  presented on a common  $0.5 \times 0.5^\circ$  grid, using a log-normal color scale.

[Title Page](#)[Abstract](#)[Introduction](#)[Conclusions](#)[References](#)[Tables](#)[Figures](#)[◀](#)[▶](#)[◀](#)[▶](#)[Back](#)[Close](#)[Full Screen / Esc](#)[Printer-friendly Version](#)[Interactive Discussion](#)

**Comparison of NO<sub>2</sub>  
in regional and global  
models to OMI**

V. Huijnen et al.

**Fig. 2.** Illustration of regions as defined in Table 2.[Title Page](#)[Abstract](#)[Introduction](#)[Conclusions](#)[References](#)[Tables](#)[Figures](#)[◀](#)[▶](#)[◀](#)[▶](#)[Back](#)[Close](#)[Full Screen / Esc](#)[Printer-friendly Version](#)[Interactive Discussion](#)

## Comparison of NO<sub>2</sub> in regional and global models to OMI

V. Huijnen et al.

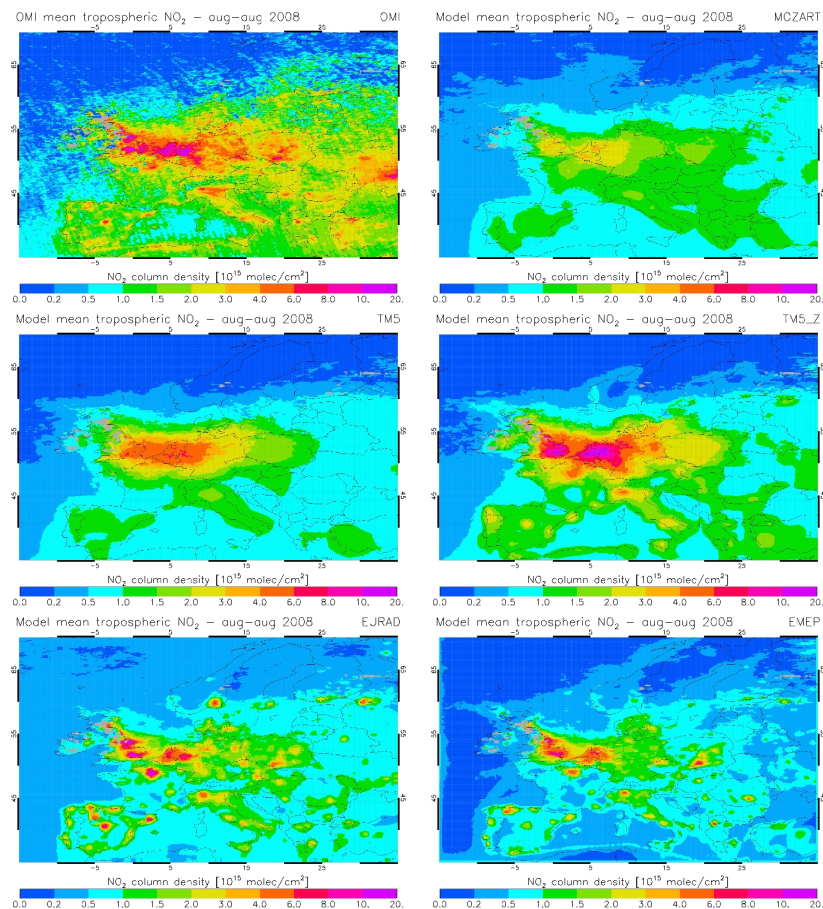


**Fig. 3.** Mean modeled tropospheric NO<sub>2</sub> columns in August for selected RAQ models, versus OMI.

Title Page

Abstract

Introduction

Conclusions

References

Tables

Figures

◀

▶

◀

▶

Back

Close

Full Screen / Esc

Printer-friendly Version

Interactive Discussion



**Comparison of NO<sub>2</sub>  
in regional and global  
models to OMI**

V. Huijnen et al.

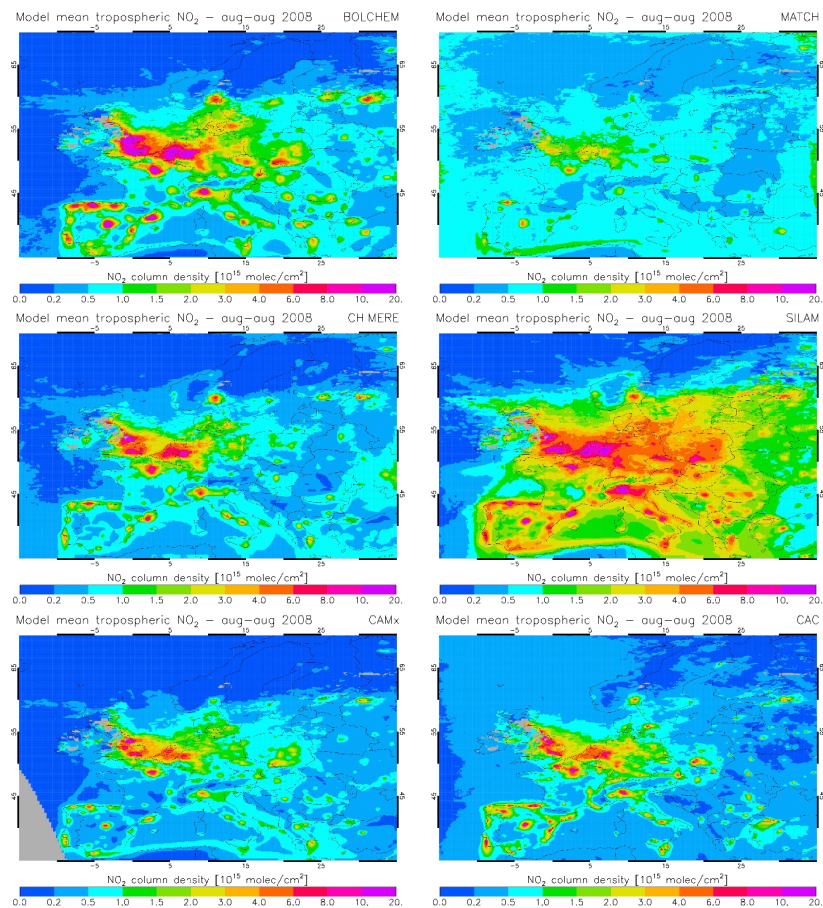


**Fig. 4.** Mean modeled tropospheric NO<sub>2</sub> columns in August for selected RAQ models, versus OMI.

Title Page

Abstract

Introduction

Conclusions

References

Tables

Figures

◀

▶

◀

▶

Back

Close

Full Screen / Esc

Printer-friendly Version

Interactive Discussion



## Comparison of NO<sub>2</sub> in regional and global models to OMI

V. Huijnen et al.

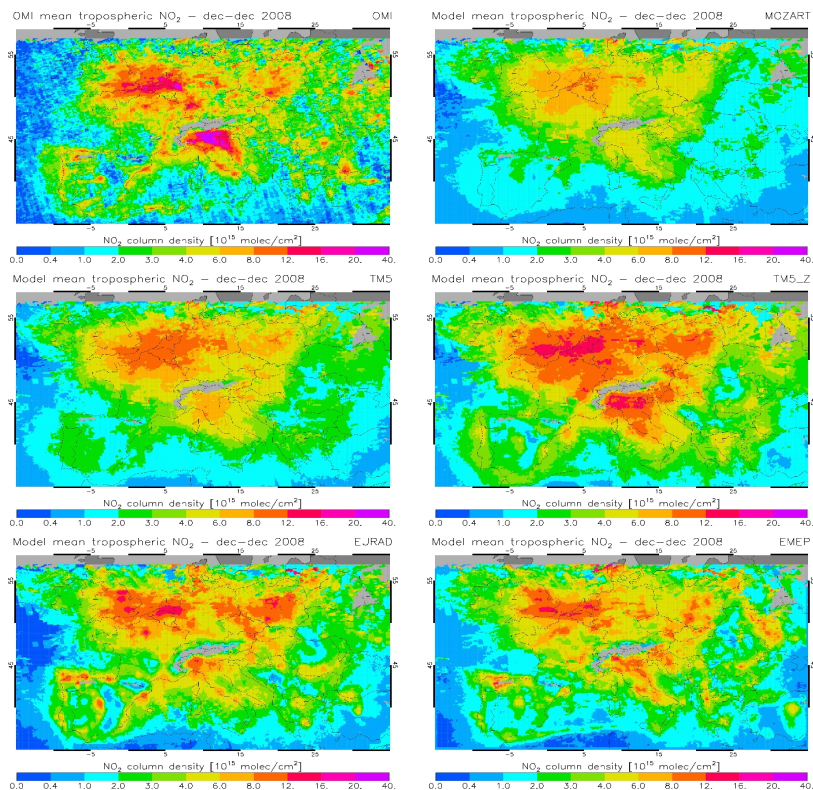


**Fig. 5.** Mean modeled tropospheric NO<sub>2</sub> columns in December for selected RAQ models, versus OMI.

[Title Page](#)[Abstract](#)[Introduction](#)[Conclusions](#)[References](#)[Tables](#)[Figures](#)[◀](#)[▶](#)[◀](#)[▶](#)[Back](#)[Close](#)[Full Screen / Esc](#)[Printer-friendly Version](#)[Interactive Discussion](#)

**Comparison of NO<sub>2</sub> in regional and global models to OMI**

V. Huijnen et al.

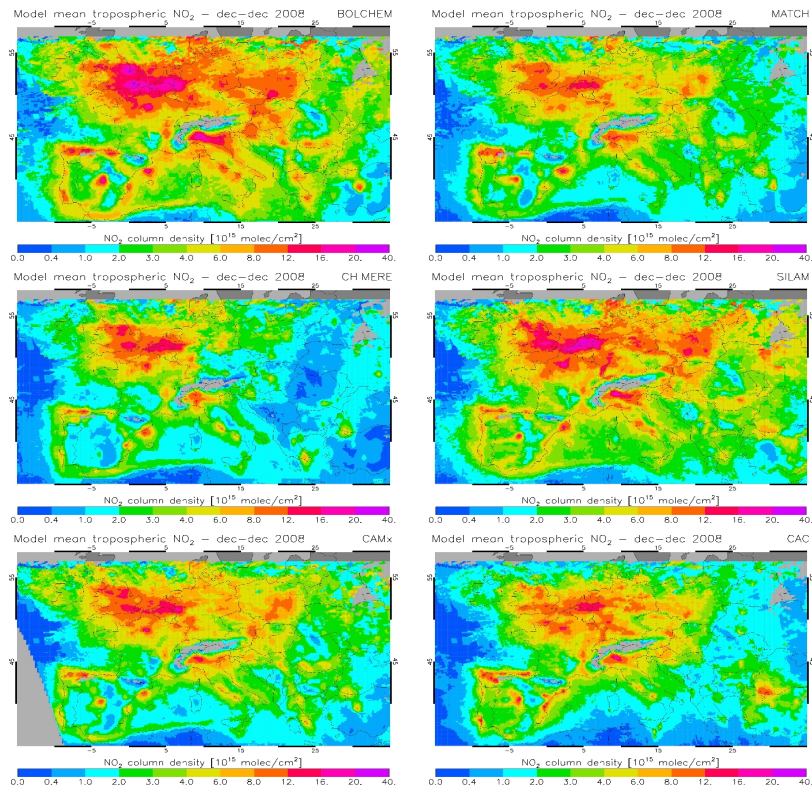


**Fig. 6.** Mean modeled tropospheric NO<sub>2</sub> columns in December for selected RAQ models, versus OMI.

[Title Page](#)[Abstract](#)[Introduction](#)[Conclusions](#)[References](#)[Tables](#)[Figures](#)[◀](#)[▶](#)[◀](#)[▶](#)[Back](#)[Close](#)[Full Screen / Esc](#)[Printer-friendly Version](#)[Interactive Discussion](#)

## Comparison of NO<sub>2</sub> in regional and global models to OMI

V. Huijnen et al.

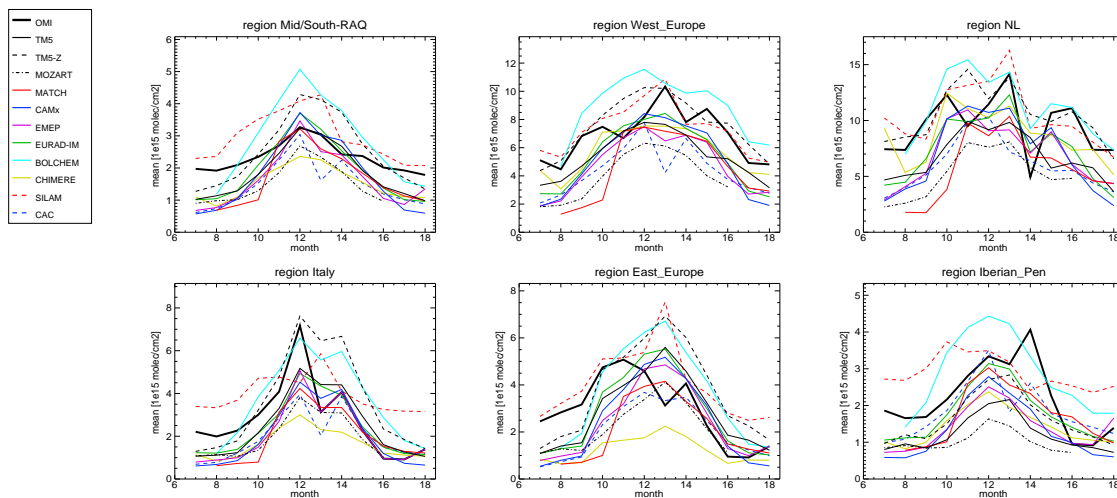


**Fig. 7.** Area-averaged monthly mean tropospheric NO<sub>2</sub> columns for selected regions, running from July 2008 (month 7) up to June 2009 (month 18).

Title Page

Abstract

Introduction

Conclusions

References

Tables

Figures

◀

▶

◀

▶

Back

Close

Full Screen / Esc

Printer-friendly Version

Interactive Discussion



## Comparison of NO<sub>2</sub> in regional and global models to OMI

V. Huijnen et al.

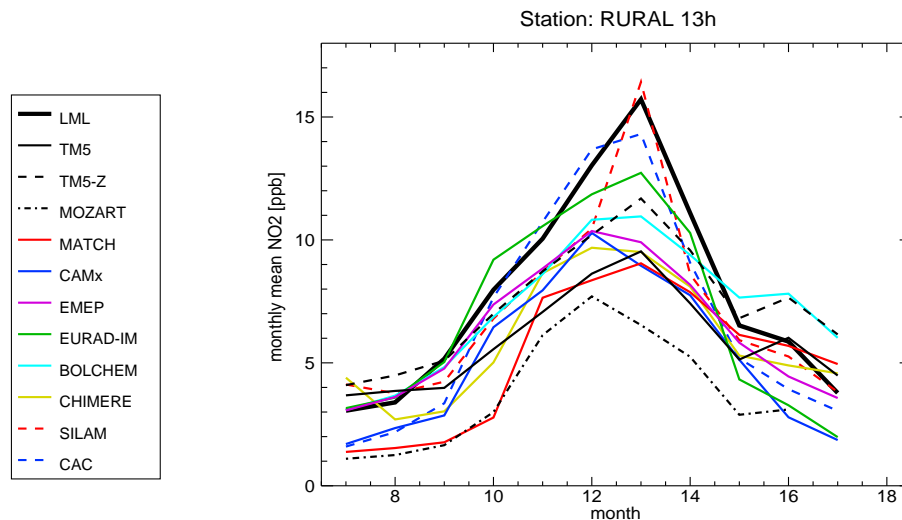


**Fig. 8.** Comparison of monthly average 13:00 UTC modeled NO<sub>2</sub> concentrations vs. Dutch LML station data corrected for the interference effect. The figures show the average concentrations from 17 rural stations.

[Title Page](#)[Abstract](#)[Introduction](#)[Conclusions](#)[References](#)[Tables](#)[Figures](#)[◀](#)[▶](#)[◀](#)[▶](#)[Back](#)[Close](#)[Full Screen / Esc](#)[Printer-friendly Version](#)[Interactive Discussion](#)

## Comparison of NO<sub>2</sub> in regional and global models to OMI

V. Huijnen et al.

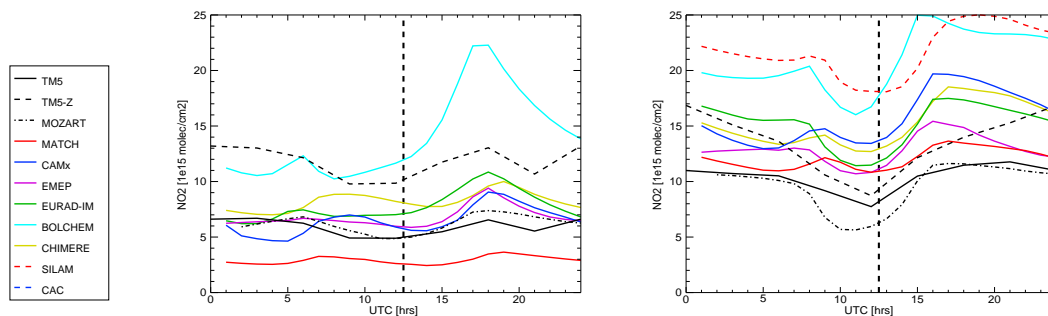


**Fig. 9.** Monthly average, diurnal cycle of NO<sub>2</sub> tropospheric columns in September (left) and December (right), over the Netherlands region. The dashed line indicates the OMI overpass-time.

[Title Page](#)[Abstract](#)[Introduction](#)[Conclusions](#)[References](#)[Tables](#)[Figures](#)[◀](#)[▶](#)[◀](#)[▶](#)[Back](#)[Close](#)[Full Screen / Esc](#)[Printer-friendly Version](#)[Interactive Discussion](#)

**Comparison of NO<sub>2</sub> in regional and global models to OMI**

V. Huijnen et al.

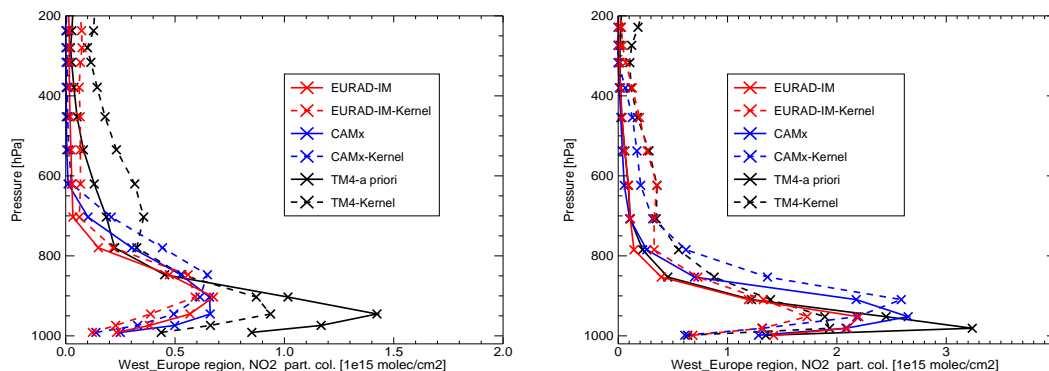


**Fig. 10.** Monthly mean, area-averaged partial NO<sub>2</sub> columns, interpolated on TM4-vertical model grid, for CAMx and EURAD-IM, as well as the partial column multiplied with the averaging kernel. Also shown the TM4 data. Results for western Europe region, August 2008 (left) and December 2008 (right).

[Title Page](#)[Abstract](#)[Introduction](#)[Conclusions](#)[References](#)[Tables](#)[Figures](#)[◀](#)[▶](#)[◀](#)[▶](#)[Back](#)[Close](#)[Full Screen / Esc](#)[Printer-friendly Version](#)[Interactive Discussion](#)

## Comparison of NO<sub>2</sub> in regional and global models to OMI

V. Huijinen et al.

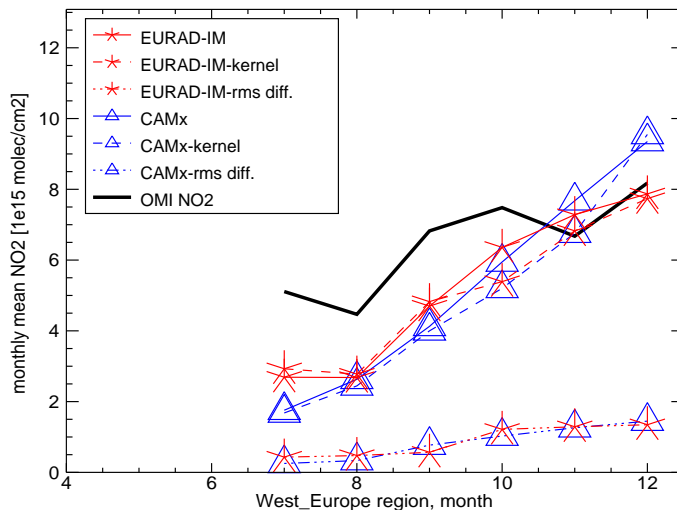
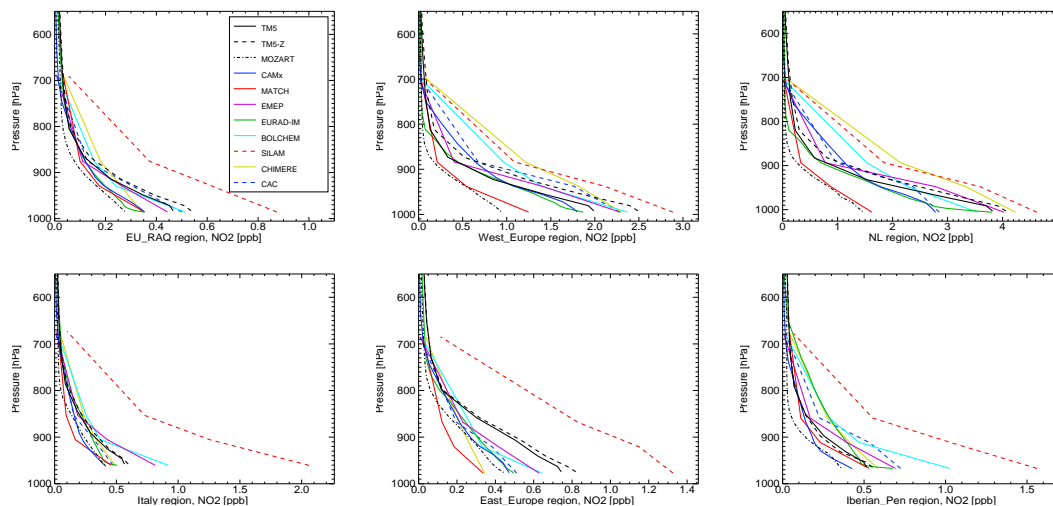


**Fig. 11.** EURAD-IM and CAMx monthly area-averaged modeled tropospheric NO<sub>2</sub> column ( $N_{tc}$ ) and the version using the averaging kernel ( $N_k$ ). Average over western Europe region. Also shown the OMI retrieval and the area-averaged rms-differences between  $N_{tc}$  and  $N_k$  for both models.

[Title Page](#)[Abstract](#)[Introduction](#)[Conclusions](#)[References](#)[Tables](#)[Figures](#)[◀](#)[▶](#)[◀](#)[▶](#)[Back](#)[Close](#)[Full Screen / Esc](#)[Printer-friendly Version](#)[Interactive Discussion](#)

## Comparison of NO<sub>2</sub> in regional and global models to OMI

V. Huijnen et al.

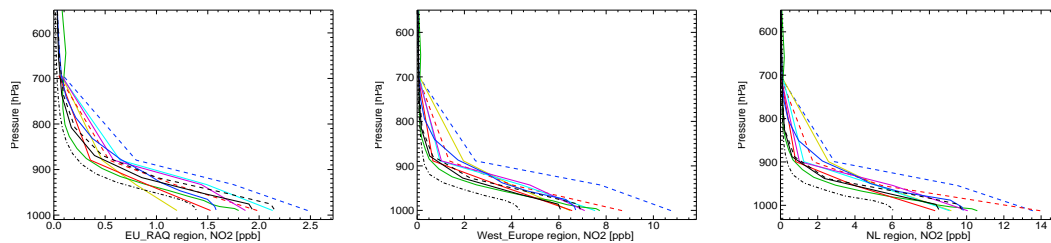


**Fig. 12.** Monthly mean, area-averaged profiles for August at 12:00 UTC. No cloud filtering is applied for these averages.

[Title Page](#)[Abstract](#)[Introduction](#)[Conclusions](#)[References](#)[Tables](#)[Figures](#)[◀](#)[▶](#)[◀](#)[▶](#)[Back](#)[Close](#)[Full Screen / Esc](#)[Printer-friendly Version](#)[Interactive Discussion](#)

**Comparison of NO<sub>2</sub> in regional and global models to OMI**

V. Huijnen et al.

**Fig. 13.** Monthly mean, area-averaged profiles for December.[Title Page](#)[Abstract](#)[Introduction](#)[Conclusions](#)[References](#)[Tables](#)[Figures](#)[◀](#)[▶](#)[◀](#)[▶](#)[Back](#)[Close](#)[Full Screen / Esc](#)[Printer-friendly Version](#)[Interactive Discussion](#)